Uncertainties and associated concerns relating to using short-term projections to advise on the 2020 sardine TAC and TABs

C.L. de Moor*, J.C. Coetzee# and D.S. Butterworth*

Correspondence email: *carryn.demoor@uct.ac.za*

The analyses undertaken to provide a scientific recommendation for the 2019 sardine TAC and TAB, under Exceptional Circumstances were subject to a number of more serious uncertainties than would normally apply. Given the critically low level of the sardine resource, care should be taken to either recommend catch limits that are robust to these uncertainties, or to undertake further research to minimise such uncertainty. One key uncertainty is how survey (and commercial) length frequencies should be weighted given that concerns frequently arise that one or other (or both) may be unrepresentative of the population length structure. Future recruitment to this short-lived resource is another key uncertainty. While the primary uncertainty surrounding the weight-at-length has been alleviated, and the growth curve adjusted, some uncertainty surrounding the choice of growth curve remains. Finally, under Exceptional Circumstances, the decision-making process involves a greater degree of subjectivity. While the Small Pelagic Scientific Working Group aimed at making this as objective as possible to recommend 2019 sardine catch limits, that approach could possibly be further improved. This document is aimed at providing current research and analyses to assist discussion on the key questions to the panel at the MARAM International Stock Assessment Workshop.

Introduction

This document discusses a number of uncertainties and concerns about the analysis and decision making process outlined for South African sardine in de Moor and Coetzee (2019 – MARAM/IWS/2019/Sardine/P2). These are listed below in roughly descending order of priority with regard to how the uncertainties may impact the analysis and decision making process expected to be followed in early 2020 to recommend sardine TAC and TABs for 2020.

Length frequencies

Hydro-acoustic surveys are conducted annually to estimate the biomass of sardine and other co-occuring pelagic fish species. A stratified random transect survey design (Jolly and Hampton 1990) is used, whereby transects are grouped into standard strata (Figure A1). Each transect comprises several intervals, typically each about 10 nm in length. Objective discrimination between co-occurring pelagic fish species having similar acoustic properties is currently not possible, particularly at night when schools disaggregate into sound scattering layers. Acoustic energy (S_A, m^2nm^{-2}), summed over each interval, is therefore apportioned to each species based on the species composition of trawl catches in the immediate vicinity of each acoustic interval. This apportioned energy is converted to fish density (Appendix A) through species-specific length-based target strength (TS) regressions (Barange *et al*. 1996, Coetzee *et al*. 2008). The length used for each acoustic interval in the conversion from acoustic energy to fish density is typically obtained from the nearest trawl that contained sardine.

TS typically increases with length due to an increase in the size of the swimbladder with length and more than 90% of the fish echo is due to the sound speed contrast between the air-filled swimbladder and the surrounding tissue and water. Various behavioural, physiological and environmental factors can cause substantial changes in the TS of fish or other acoustic targets and for this reason an average TS at length is typically used. Incorporating the mean weight of fish of a particular length into the TS

* MARAM (Marine Resource Assessment and Management Group), Department of Mathematics and Applied Mathematics, University of Cape Town, Rondebosch, 7701, South Africa.

Department of Environment, Forestry and Fisheries, Private Bag X2, Vlaeberg 8018, Cape Town, South Africa.

regression, either through a known W/L relationship or through the actual mean weight of fish measured at the time that the TS was measured, enables the conversion from $TS.ind^{-1}$ to TS kg^{-1} where these TS regressions then represent the amount of energy reflected by 1 kg of fish of a certain species and length (Figure A2). It is important to note here that the *TS* kg^{-1} regression retains its dependence on fish length and that such TS regressions could potentially be adjusted for fish condition through the use of an alternative L/W regression in situations where such additional information is available. For small pelagic fish biomass surveys conducted in South Africa, however, a constant TS kg^{-1} expression is used based on a regression between mean TS kg^{-1} and mean fish length, where TS kg^{-1} at length was derived for each individual TS measurement by dividing the TS ind^{-1} at length by the mean weight of fish that contributed to the mean length distribution at the time of the TS measurement.

There is some concern that the November 2018 survey length frequency may have under-represented large sardine (Appendix D of de Moor and Coetzee 2019 – MARAM/IWS/2019/Sardine/P2), which may have led to an inaccurate determination of sardine biomass, length frequency and mean weight of fish. The impact of such possible under-sampling was estimated in April 2019 (Coetzee 2019) for a single stratum and subsequently for the area to the west and east of Cape Agulhas (de Moor and Coetzee 2019 – MARAM/IWS/2019/Sardine/P2), based on an average proportion at length of commercial catches taken during October-December 2018 and survey samples west and east of Cape Agulhas. This suggested that the sardine biomass could potentially have been underestimated by up to 65% west of Cape Agulhas and by up to 35 % east of Cape Agulhas. The corresponding effect on number of sardine was a decrease of 48% west of Cape Agulhas and a decrease of 35% east of Cape Agulhas. This extent of change in biomass and number of fish was suggested as an upper bound because the combined length frequency would be unrepresentative of small sardine given that industry would, according to permit conditions, avoid targeting sardine < 14 cm Lt (~12 cm Lc).

Length frequencies obtained from surveys and commercial catches taken between October and November (coinciding with the timing of the survey) in the area to the west and east of Cape Agulhas each year since 2009, were plotted in an attempt to understand whether large sardine may also have been under-sampled in previous surveys (Appendix B). There is good overlap in the range of commercial and survey length frequencies in several years with the higher proportion of larger fish in the commercial catches being explained by the lack of small sardine (< ~14cm). In some years, including 2018, any mode present at larger lengths in the commercial catch is either not very clear in the survey data, or completely absent, suggesting under-sampling of large sardine by the survey. Under-sampling of large sardine may arise from their faster swimming speed and hence their greater ability to avoid the survey trawl gear. Ultimately some relative weighting, rather than simply averaging commercial and survey length frequencies will be required if the survey length frequencies, are to be adjusted to estimate the survey biomass and number of fish more accurately, particularly in years where length distributions appear anomalous.

Thought should be given to how such a weighting factor could be incorporated, particularly if it is to be done at the interval level, as any changes to the sardine length frequency will result in an altered density for that interval (see equation A3 in Appendix A), transect, stratum and total survey area as well as in the estimate of precision (CV) not only of sardine, but also of other co-occurring species though the impact on other species is likely small. An example of this is shown in Appendix C, where the original survey weighted length frequency for sardine west and east of Cape Agulhas, is used at the interval level (instead of the original trawl length frequency) for the calculation of density. A further consideration when implementing such a regional-adjusted length frequency is that small sardines are mainly found inshore. Where individual trawls under-sample large sardine, the species composition will also be under-representative of sardine and lead to an overestimation in the biomass of other species present in the catch.

As a further means to take into account the greater reliability of survey length frequencies in some years over others, sensitivity to the assessment model is tested with the standard deviation used in the likelihood for survey proportion-at-length data estimated annually instead of over all years (Equation D34, Table D1). For this sensitivity, a higher standard deviation is estimated for November 2018, effectively down-weighting this length frequency (Figure 1).

Survey data

A further complication arises from the uncertainty surrounding the November 2018 survey length frequency. There was no hydro-acoustic survey of small pelagic recruitment in May/June 2018. The model estimate of November 2017 recruitment is therefore primarily informed by the November 2018 survey length frequency. If larger fish were under-represented in this length frequency, the November 2017 / May 2018 recruitment would have been over-estimated (see Figure 4 of de Moor and Coetzee (2019) – MARAM/IWS/2019/Sardine/P2). Note that the model estimated recruitment in November 2017 was relatively high compared to recent years (Figure 2), and that the model predicts a higher biomass in November 2018 than that observed (Figure E1).

Stock-recruitment relationship

Operational Management Procedures for South African sardine (and anchovy) have been tuned using Operating Models with future recruitment generated from a stock-recruitment relationship. For OMP-18 (de Moor 2018a), west component recruitment was generated as:

$$N_{west,y,0}^{pred} = \begin{cases} a_{west} e^{\varepsilon_{west,y}\sigma_{west,r}} & if\ SSB_{west,y}^{eff} \geq b_{west} \\ a_{west} \frac{SSB_{west,y}^{eff}}{b_{west}} e^{\varepsilon_{west,y}\sigma_{west,r}} & if\ SSB_{west,y}^{eff} < b_{west} \end{cases}$$

where

$\varepsilon_{west,y} = s_{west,cor}\varepsilon_{west,y-1} + \omega_{west,y}\sqrt{1-\left(s_{west,cor}\right)^2}$, where $\omega_{west,y} \sim N(0,1)$

The parameters for this hockey-stick stock recruitment relationship were estimated by excluding the 'pulse years' of 2000-2004 (Figure 3). The south component recruitment was generated from a "two step" model (Figure 4), independent of spawner biomass (de Moor 2018b):

$$ln\left(N_{southy,0}^{pred}\right) = \begin{cases} u_1 + \epsilon_{1,y} & if\ \varepsilon_{south,y} < p \\ u_2 + \epsilon_{2,y} & if\ \varepsilon_{south,y} \geq p' \end{cases}$$

where $\varepsilon_{south,y} \sim Random[0,1]$, $\epsilon_{1,y} \sim N(0,\sigma_1^2)$ and $\epsilon_{2,y} \sim N(0,\sigma_2^2)$.

For the baseline short term projections used in early 2019 (de Moor and Coetzee 2019 – MARAM/IWS/2019/Sardine/P2), recruitment was drawn at random with replacement from that estimated for the most recent 5 years, under the assumption that future recruitment, particularly in the immediate short-term future, may be from a similar "regime" to that for the recent past (Figure 3 of de Moor and Coetzee 2019 – MARAM/IWS/2019/Sardine/P2). The most recent 5 or 10 years are frequent choices for the "recent past" in projection analyses internationally. Figure 2 gives an updated recruitment time series corresponding to Appendices D and E, and it is proposed that any short term projections in 2020 use recruitments generated from the values estimated by next year's assessment (including 2019 data) for November 2014-2018 (though noting the possibility that November 2017 may be poorly estimated, see above).

Figure 5 shows hockey-stick stock recruitment curves fit to the model estimates of "effective" spawning biomass and recruitment, assuming 8% of south coast spawning biomass contributes to west coast effective spawning biomass. The years 2000-2004 have previously been defined as the 'pulse years', and were excluded from any stock-recruitment relationships for the total population and for the west component sardine. However, these years were selected some time ago as those corresponding to peak spawning biomass when the population was still considered to be a single homogeneously mixed stock (Figure 6), and these five years no longer correspond to the highest west component effective spawning biomass (Figures 5 and 6). It is therefore suggested that for future OMP developments, west component stock-recruitment relationships are estimated from all data, excluding only 2000-2002 as 'pulse years' (based on the recruitment, rather than the spawner biomass estimated in these years), while the south component recruitment continues to be generated by the "two-step" model appropriately adjusted to correspond to updated Operating Models.

A complication arising from the spawner biomass hinge point being estimated to be relatively low (note the hinge point in Figure 5 has been lower given different model assumptions), together with the model estimating the west component recruitment to be the primary driver of population dynamics, is that projections based on such a curve would indicate that the resource could be harvested to a low level without any negative impact on expected median recruitment. Given the currently very low level of sardine biomass (see 2018 spawner biomass in Figure 5; again note that for other model assumptions the hinge point is near this 2018 spawner biomass), the need for caution and careful estimation is obvious.

<u>Basis for making short-term management recommendations</u>

The sardine population is currently at its lowest observed level, corresponding to that surveyed ~35 years ago, and Exceptional Circumstances have been declared. The primary objective of the SWG-PEL in providing management advice is now to therefore "assist the speedy recovery of sardine to a higher biomass level". However, the socio-economic implications of any management recommendations also need to be considered. For this reason the directed sardine fishery was not closed in 2019. In addition, severely constraining the small sardine bycatch with anchovy could hamper the anchovy fishery, which has consistently had high TACs in recent years in response to high anchovy abundances.

The SWG-PEL decided to recommend catch limits that would result in the 20%ile of projected November 2019:2018 west component effective spawning biomass being 80% of that under a no-2019-catch scenario. The one-year-only projections in these analyses (with incoming recruitment contributing substantially to the biomass projected) together with the short-lived, highly variable characteristics of sardine, meant a direct comparison to the decision making process followed for West Coast Rock Lobster (Johnston and Butterworth 2016) – also under Exceptional Circumstances - was problematic. The 80% was selected after initial results were available, attempting to take into account that this depletion estimate is the impact of a single year's catch and the importance of sardine as a key forage species for natural predators in the ecosystem. Such a strategy would allow for some (small) catch no matter how low the population size. This is in contrast to, for example, the Californian sardine fishery where fishing is stopped once biomass falls below a cut-off threshold.

The sardine TAC has been substantially under-caught for the past 3 years, which is a further indication of the poor stock status of sardine (Figure 7). During 2019 the directed sardine catch has totalled <1000t to date, just 8% of the TAC awarded after the process outlined by de Moor and Coetzee (2019 – MARAM/IWS/2019/Sardine/P2).

Growth

While the impact of alternative 2019 catch limits was considered under both a cohort growth curve (where the length at age in year y depends on $t_{0,j,y-a}$) and an annual growth curve (where the length at age in year y depends on $t_{0,j,y}$), the annual growth curve is now no longer considered realistic. The range of $t_{0,j,y}$'s estimated during the initial 2019 assessment was unrealistically large, spanning approximately a year. The normal prior distribution on the residuals about the age at which the length is zero has been substantially reduced (Table D1). Having constrained the range of $t_{0,j,y}$'s to approximately 7 months (which may still be unrealistically wide), the average $t_{0,j=1,y}$ has shifted to approximately April (early recruitment) for the west component (Figure E10). The peak spawning period of sardine off the West Coast (based on GSI values) is from August to February with a peak in December (van der Lingen and McGrath 2017). While noting the interpretation of $t_{0,j,y}$ is not precise given growth during the early life stages of a fish may not follow the von Bertalanffy growth curve shape, an average $t_{0,j=1,y}$ of April may, nevertheless be considered unrealistic. Two alternative growth curves have been tested, whereby the slope parameter κ is increased to 1.2κ for i) ages < 1 and ii) ages < 6 months. Continuity and derivative continuity is maintained at this age-hinge-point. These two alternatives result in a smaller range of $t_{0,j,y}$'s and averages closer to November (Figure 8). However, the age-hinge-point of 1 results in a much poorer fit to the parasite prevalence-at-length data (Table 1). The age-hinge-point of 6 months, however, does not result in a substantially worse fit to any of the data sets, and offers an improved fit over the current baseline to some data sets.

Maturity/selectivity-at-age from maturity/selectivity-at-length

Equations D14-16 detail the use of selectivity-at-length in the age-structured assessment. This selectivity-at-length is converted to selectivity-at-age for use in simulating the impact of catches in Equations D15 and F4. Although not used in these short-term projections, other projection analyses have similarly used maturity-at-age calculated from maturity-at-length (Table D1).

While the use of a length-at-age distribution (Figure E11) to convert from age to length is straightforward, the assumption that the 'reverse conversion' from length to age is accurate has been questioned. For example, neither selectivity-at-age 5+ nor maturity-at-age 5+ is estimated to be 1 (Figure 9). While selectivity-at-age is standardly renormalized prior to use in any projections, maturity-at-age is not, and there is some concern that this resultant maturity-at-age may bias projection analyses.

Sardine weight-at-length

The "initial 2019 assessment" of de Moor (2019a) adjusted the November weight-at-length annually, informed by the average weight of sardine sampled during the survey, to account for the differing condition factor of sardine at the time of the survey. Short-term projections varied substantially depending on whether the recent average condition factor was assumed, or whether the low condition factor associated with the November 2018 survey was assumed (se Moor 2019b). This uncertainty received a low weight by the time decisions based on de Moor and Coetzee (2019 – MARAM/IWS/2019/Sardine/P2) were made, given the condition factor observed in early 2019 (van der Lingen *et al*. 2019).

Recent discussions have clarified that the hydro-acoustic survey estimate of total biomass depends on the size of the fish swim bladder which depends (through a time invariant target strength relationship) on fish length only, and not on the condition (skinniness/fattiness) of the fish at the time of the survey. A time-invariant weight-at-length therefore provides the most appropriate basis to estimate biomass from the population model to correspond to the time series of biomasses from the survey (which is independent of sardine condition factor) and is now used in the assessment (Appendix D). Any short-term projections during 2020 should, therefore, not be subject to this uncertainty.

References

Barange M, Hampton I, Soule M. 1996. Empirical determination of *in situ* target strengths of three loosely aggregated pelagic fish species. ICES Journal of Marine Science 53: 225–232.

Coetzee JC, Merkle D, de Moor CL, Twatwa NM, Barange M, Butterworth DS. 2008. Refined estimates of South African pelagic fish biomass from hydro-acoustic surveys: quantifying the effects of target strength, signal attenuation and receiver saturation. African Journal of Marine Science 30(2): 205-217.

Coetzee J. 2019. Potential bias in November survey biomass estimates as a result of suspected under catch of larger sardine. DAFF: Branch Fisheries Document FISHERIES/2019/APR/SWG-PEL/09.

de Moor CL. 2016. The two mixing stock hypothesis for South African sardine without an assumed stock-recruit relationship. DAFF: Branch Fisheries Document FISHERIES/2016/NOV/SWG-PEL/57.

de Moor CL. 2018a. The 2018 Operational Management Procedure for the South African sardine and anchovy resources. DAFF: Branch Fisheries Document FISHERIES/2018/DEC/SWG-PEL/37.

de Moor CL. 2018b. Simulation testing framework used during OMP-18 development. DAFF: Branch Fisheries Document FISHERIES/2018/SEP/SWG-PEL/27.

de Moor CL. 2019a. Revision to the Initial Assessment of the South African sardine resource using data from 1984-2018. DAFF: Branch Fisheries Document FISHERIES/2019/MAR/SWG-PEL/06.

de Moor CL. 2019b. Sardine projections based on constant catch scenarios. DAFF: Branch Fisheries Document FISHERIES/2019/APR/SWG-PEL/07.

de Moor CL. 2019c. Progress towards updating the assessment of the South African sardine resource using data from 1984-2018. DAFF: Branch Fisheries Document FISHERIES/2019/NOV/SWG-PEL/29.

de Moor CL, Bergh M, Butterworth DS, Coetzee JC and van der Lingen CD. 2018. Density dependent movement of South African sardine. DAFF: Branch Fisheries Document FISHERIES/2018/FEB/SWG-PEL/02.

de Moor CL and Butterworth DS. 2016. Assessment of the South African sardine resource using data from 1984-2015: Results at the joint posterior mode for the two mixing stock hypothesis. DAFF: Branch Fisheries Document FISHERIES/2016/JUL/SWG-PEL/22REV2.

de Moor CL and Coetzee JC. 2019. A summary of the method used to provide 2019 catch limit advice for South African sardine. MARAM International Stock Assessment Review Workshop, 2-6 December 2019. MARAM/IWS/2019/Sardine/P2.

de Moor CL, Merkle D, Coetzee J and van der Lingen C. 2019. The data used in the 2019 sardine assessment. DAFF: Branch Fisheries Document FISHEREIS/2019/SEP/SWG-PEL/22.

Johnston SJ and Butterworth DS. 2016. Further projections of the west coast rock lobster resource for a range of future constant catch and poaching scenarios. DAFF: Branch Fisheries Document FISHERIES/2016/AUG/SWG/WCRL/32.

Jolly GM, Hampton I. 1990. A stratified random transect design for acoustic surveys of fish stocks. Canadian Journal of Fisheries and Aquatic Sciences. 47(7): 1282–1291.

Szuwalski CS, Britten GL, Licandeo R, Amoroso RO, Hilborn R and Walters C. 2019. Global forage fish recruitment dynamics: A comparison of methods, time-variation, and reverse causality. Fisheries Research 214: 56-64.

van der Lingen CD, Fréon P, Fairweather TP, van der Westhuizen JJ. 2006. Density-dependent changes in reproductive parameters and condition of southern Benguela sardine *Sardinops sagax*. African Journal of Marine Science 28(3&4): 625-636.

van der Lingen CD and McGrath A 2017. Incorporating seasonality in sardine spawning into estimations of the transport success of eggs spawned on the South Coast to West Coast nursery area. DAFF: Branch Fisheries Document FISHERIES/FEB/2017/SWG-PEL/08.

van der Lingen CD, Petersen J and Merkle D. 2019. Is sardine weight-at-length in 2019 lower than average? DAFF: Branch Fisheries Document FISHERIES/2019/APR/SWG-PEL/10.

Table 1. The contributions to the posterior distribution for the current baseline assessment (Appendix D) and two alternatives which change the growth curve for i) ages < 1 and ii) ages < 6 months.

	-ln(Posterior)	-ln(Likelihood)						-ln(Prior)				
		Total	Nov	Rec	Com Prop-at-length	Survey Prop-at-length	Prev-at-length	k_{ac}^{S}	$move_{1,y}$	η_y^t	$\bar{l}_{1,y}$	Penalty
Baseline	981.3	913.4	60.6	39.7	-432.2	-383.4	1628.7	-1.4	-30.3	-15.4	114.5	0.5
Alt i)	1018.9	954.4	57.7	38.0	-433.1	-388.0	1679.7	-1.3	-30.3	-17.9	114.0	0.0
Alt ii)	954.5	894.2	54.5	40.5	-428.3	-396.0	1623.5	-1.4	-30.3	-22.2	114.0	0.3

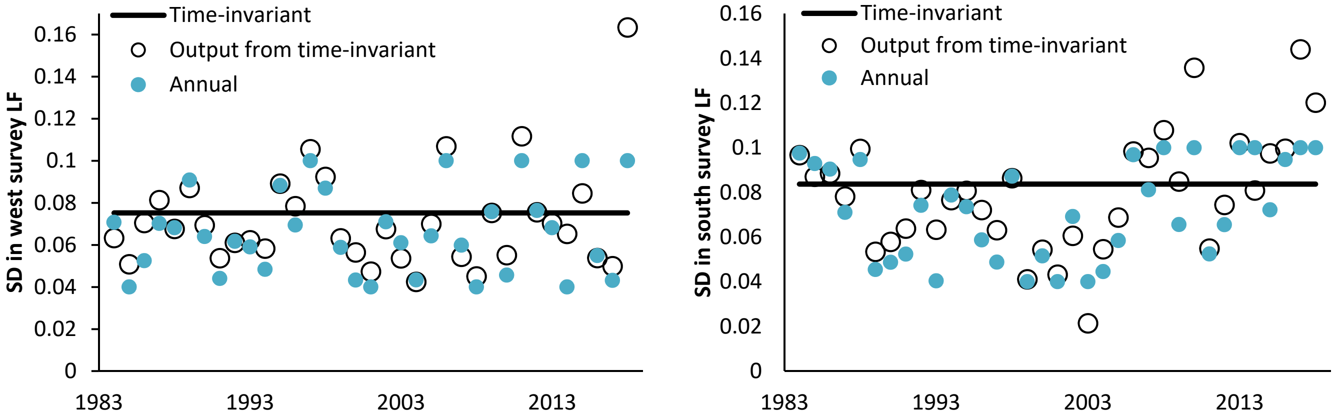

Figure 1. The time series of standard deviations associated with the survey length frequencies as calculated over all years (Appendix D), calculated annually based on the output of that run ("σ out") and calculated annually during conditioning, but constrained between [0.04,0.1].

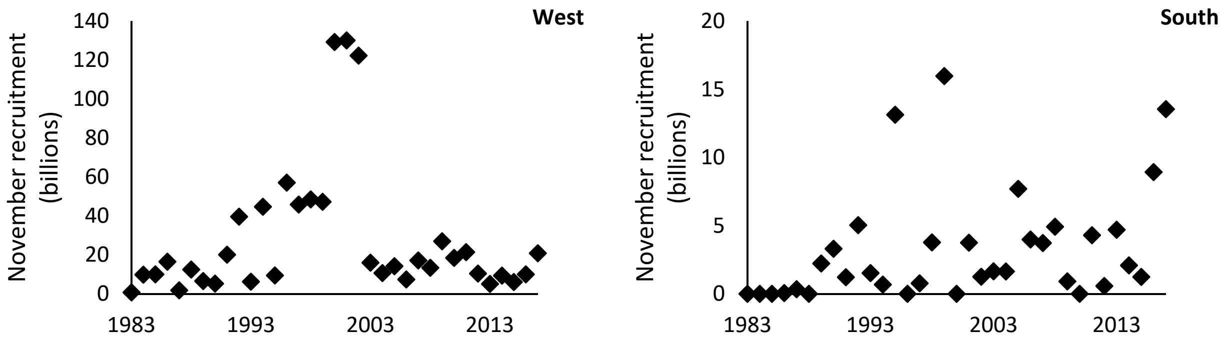

Figure 2. The model predicted November recruitment to the west and south components.

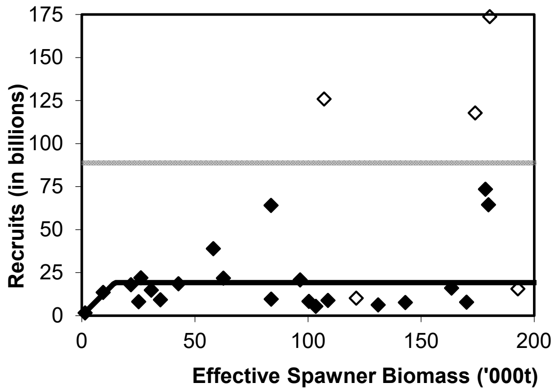

Figure 3. The 1983-2014 model estimated west component effective spawning biomass and November recruitment to the sardine resource (de Moor 2016), with a hockey-stick stock recruitment relationship fit after conditioning to the non-pulse years. The pulse years assumed (2000-2004) are shown by open diamonds.

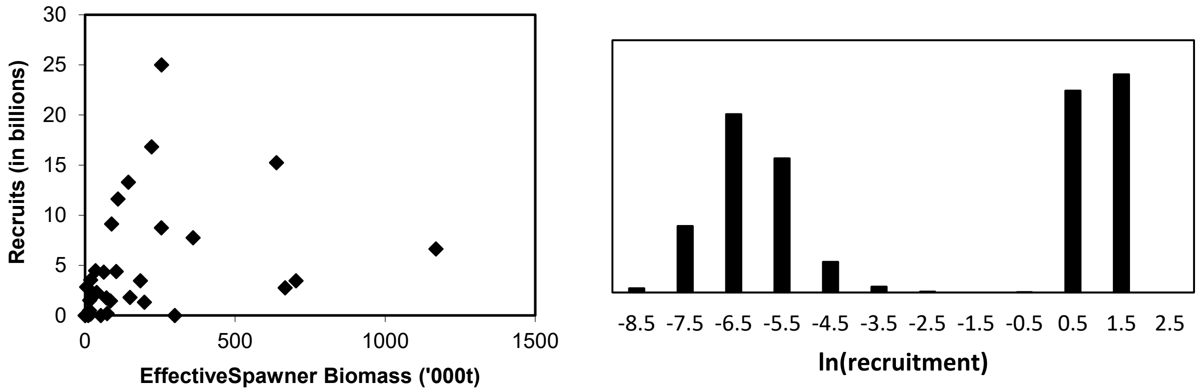

Figure 4. The 1983-2014 'best fit' model estimated south component effective spawner biomass and November recruitment to the sardine resource (de Moor 2016). Note the scale of recruitment is an order of magnitude lower than that for the west component above. The right plot shows the two distributions of log(recruitment) that were sampled from for 'normal' (u_1) and 'good' (u_2) recruitment to the south component when projecting future recruitment during OMP-18 testing.

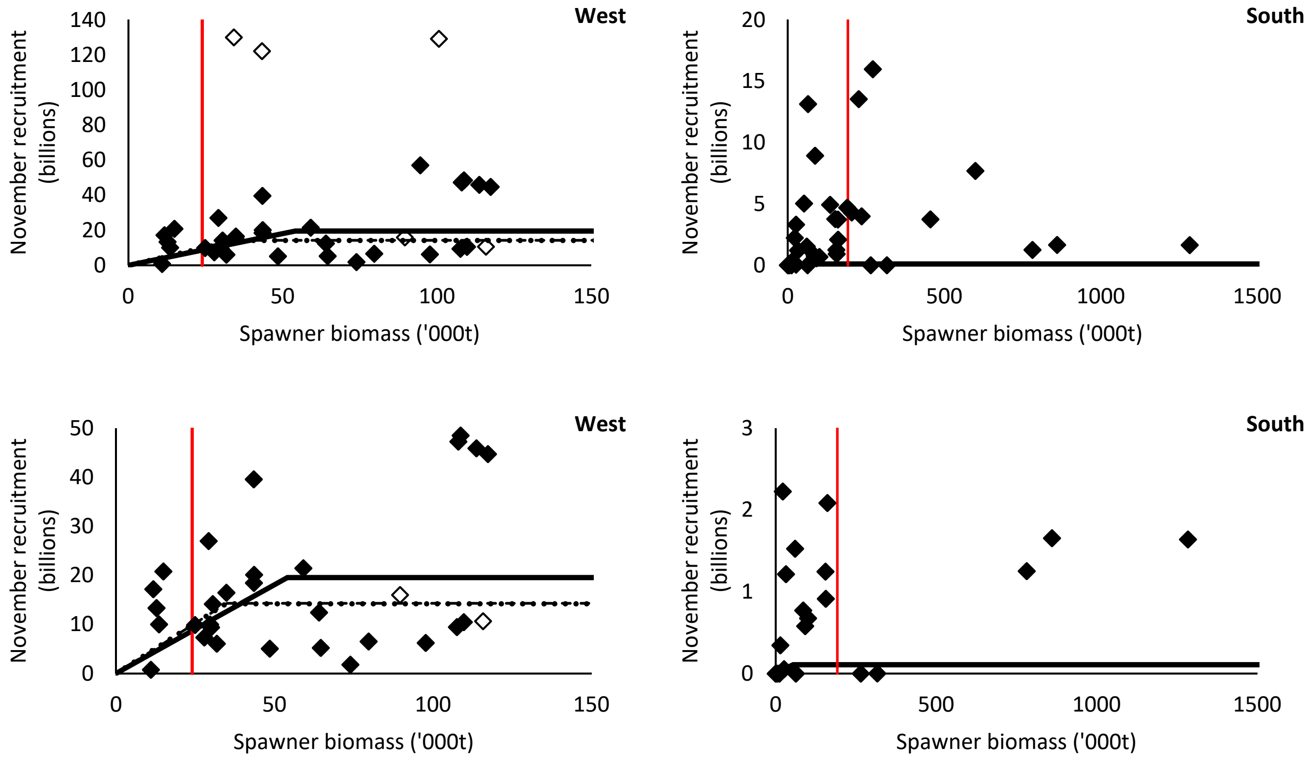

Figure 5. Hockey-stick stock recruitment curves fit to the current model estimates of "effective" spawning biomass and November recruitment, assuming 8% of south coast spawning biomass contributes to west coast effective spawning biomass. Separate curves are fit to the west data for i) all years (solid line), ii) excluding 2000-2004 (dashed line) and iii) excluding 2000-2002 (dotted line). The effective spawning biomass estimated for 2018 is indicated by the red line. The lower plots are a repeat of the upper plots, but over a smaller vertical axis range.

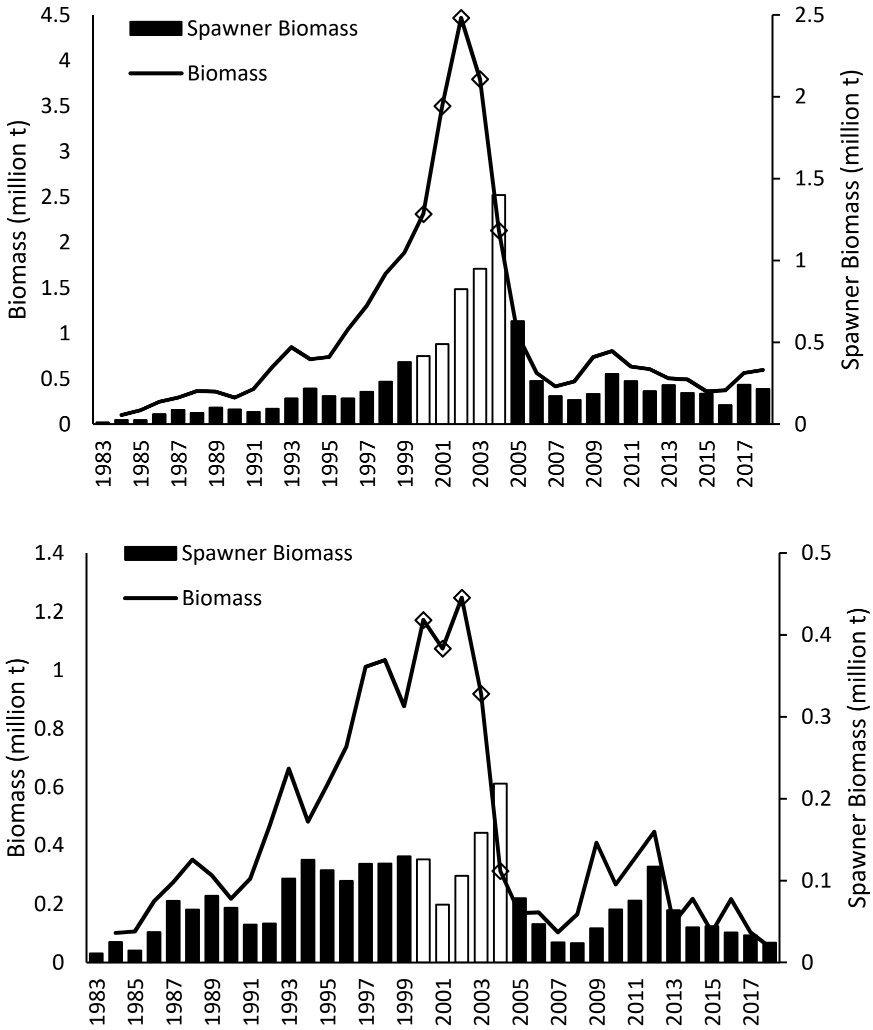

Figure 6. The total (west + south) (top) and west component (bottom) current model estimated biomass and spawning biomass, with 2000-2004 indicated by open bars/diamonds.

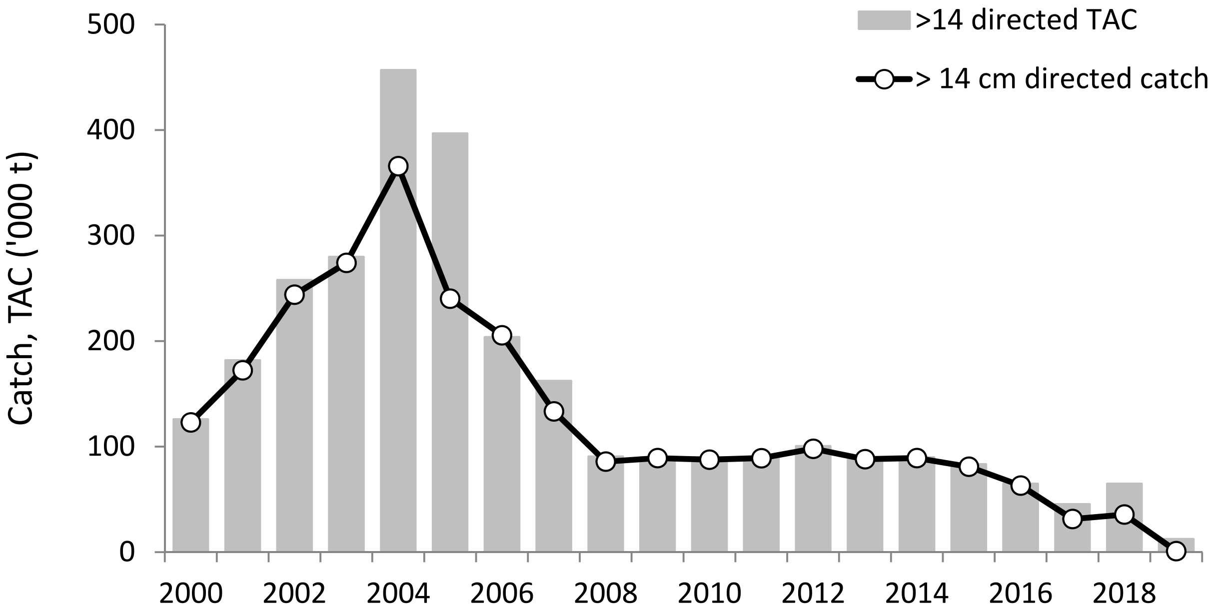

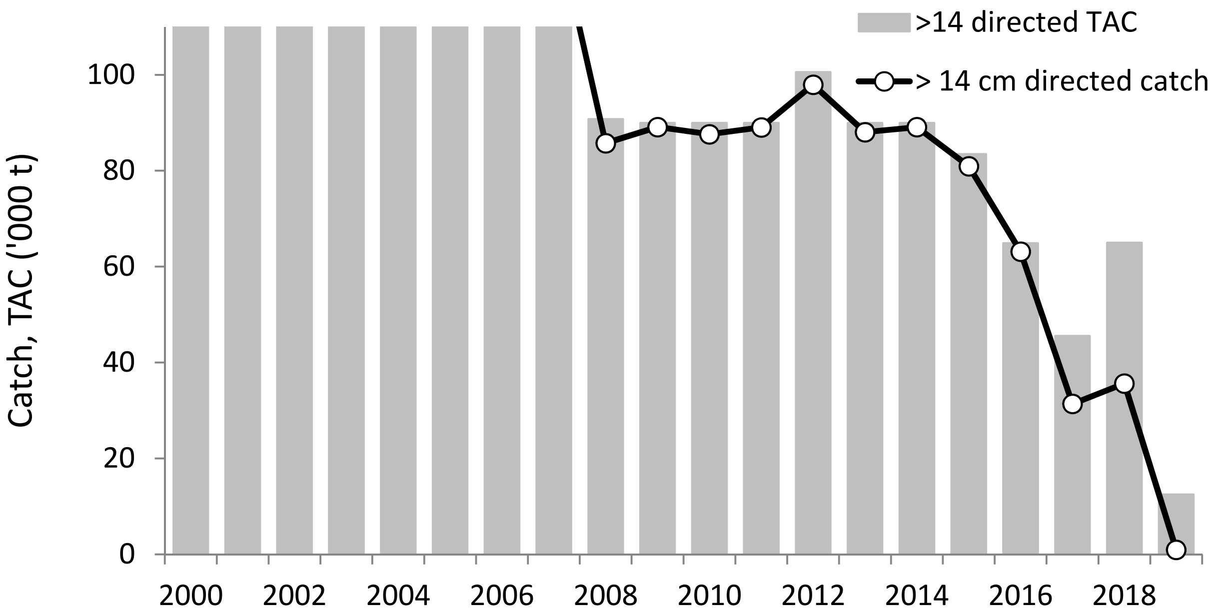

Figure 7. Directed >14cm sardine TAC and corresponding catches. 2019 catch up until 18th November 2019. The lower plot is a repeat of the upper plot, but over a smaller vertical axis range.

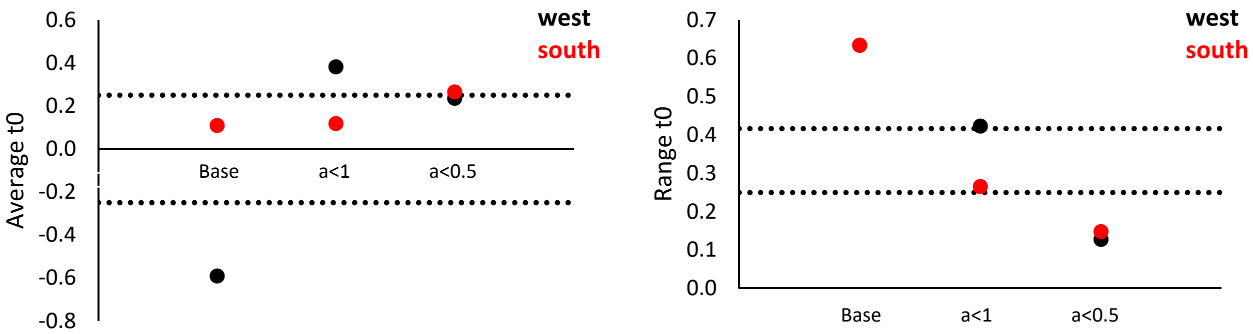

Figure 8. The average (left) and range (right) of the$t_{0,j,y}$'s estimated for the current baseline assessment (Appendix D) and two alternatives which change the growth curve for i) ages < 1 and ii) ages < 6 months. The dotted lines indicate average $t_{0,j,y}$'s of August (3 months "early") to February (3 months "late) and a range of 3 to 5 months.

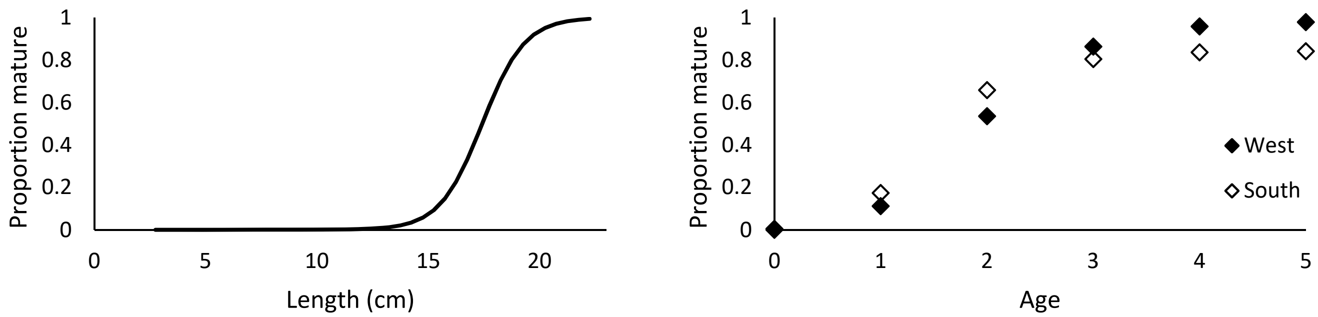

Figure 9. Maturity-at-length and maturity-at-age corresponding to the current baseline (Appendices D and E).

Appendix A: Hydro acoustic estimation of biomass

Target species of the same genus are generally not acoustically distinguishable. Echo-integrated energy per interval (section of transect; see Figure A1) is therefore allocated to different species based on the composition and length frequency distributions of trawl samples taken in the immediate vicinity. When more than one species of fish (of varying TS) is present within an interval, it is necessary to partition the echo intensity between the species, taking into account the weight of each species in the sample and their differential length-based TS regressions.

Barange *et al*. (1996) estimated target strengths for three of the South African pelagic fish species based on regression of $(TS_{kg})_j$ against mean total length (TL) of species *j* of the following form:

$$\left(TS_{kg}\right)_j = a_j + b_j log_{10}\left(TL_j\right) \qquad \text{(A1)}$$

where for anchovy TS_{kg} = -21.12 – 12.15 $\log_{10}$ (TL),
for sardine TS_{kg} = -13.21 – 14.90 $\log_{10}$ (TL),
for horse mackerel TS_{kg} = -7.75 – 15.44 $\log_{10}$ (TL).

For species *j*, this expression is converted to the linear form$(\bar{\sigma}_{bs})_j$; the mean back scattering cross section per kg which is used in equation (A3) for density estimation as follows:

$$(\bar{\sigma}_{bs})_j = \frac{\sum_{li}\left[n_{li}^j\left(10^{(0.1)a_j}\right)\left(l_i^{\frac{b_j}{10}}\right)\right]}{\sum_{li} n_{li}^j} \qquad \text{(A2)}$$

where l_i = length class, n_{li}^j = number of fish of species *j* in length class l_i ; a_j and b_j are constants in the TS_{kg} versus length relationship

The area density (*kg m*$^{-2}$) for fish of species *j* is then given by:

$$\rho_j = \frac{w_j . S_A}{4\pi . 1852^2 \sum_j^n W_j (\bar{\sigma}_{bs})_j} \qquad \text{(A3)}$$

where w_j is the weight of species *j* in the trawl sample and S_A is the total nautical area scattering coefficient attributed to all species present in the interval.

Interval density per species is then averaged per transect and per stratum to derive a mean density per stratum, which when scaled up to the stratum area results in a biomass per species per stratum (Jolly and Hampton 1990). Summation of biomass per species per stratum gives the total biomass per species.

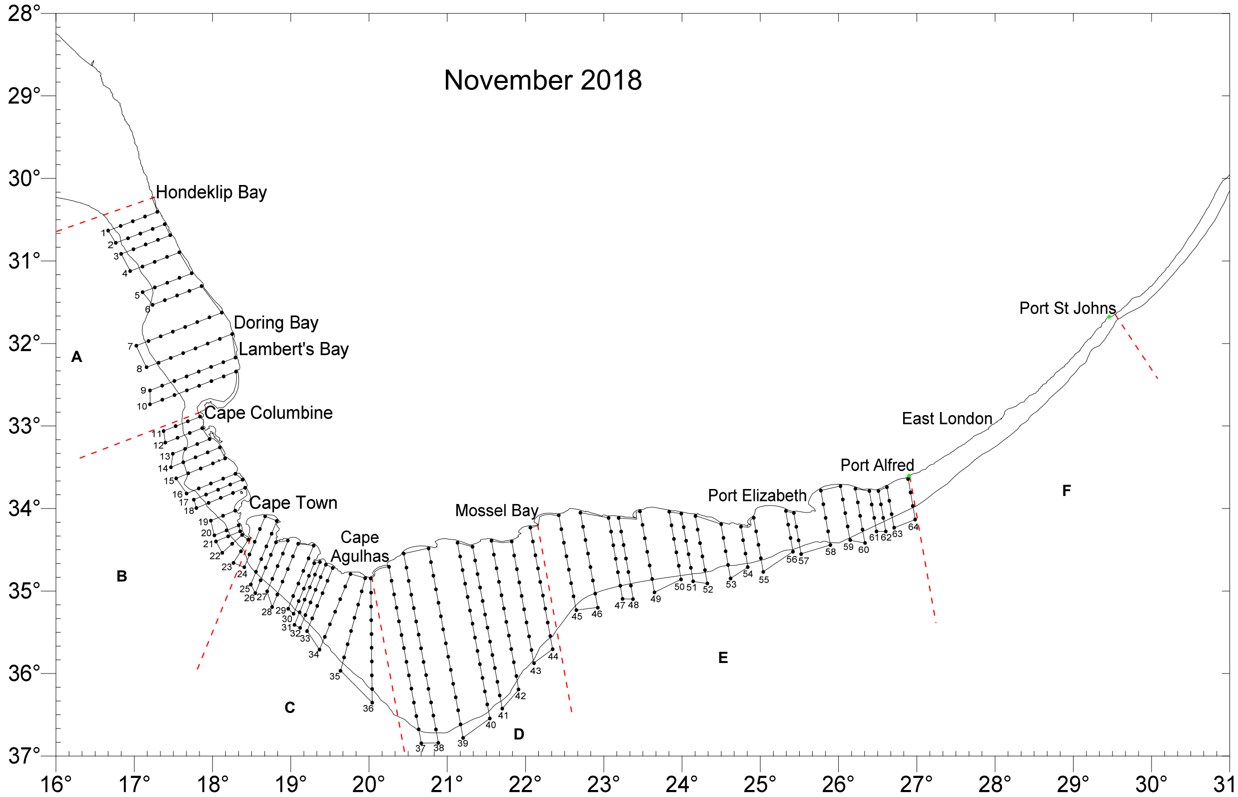

Figure A1. Typical survey design showing acoustic intervals (between dots on transects), transects and stratum boundaries.

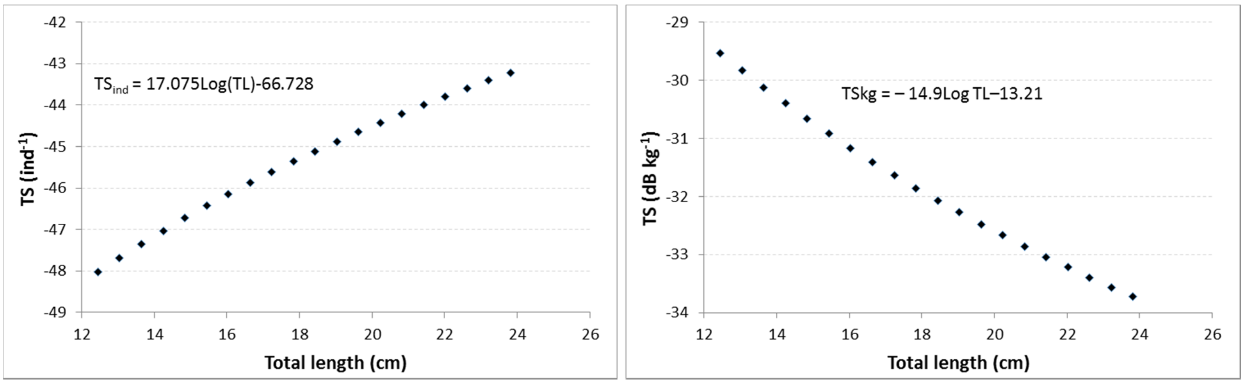

Figure A2. The relationship between target strength TS ind^{-1} and total length (left) and between TS kg^{-1} and total length (right) for sardine. The conversion from TS at length to TS at weight is based on the actual mean weight of fish of a certain mean length as recorded at the time of the TS experiments (Barange *et al*. 1996).

Appendix B: A comparison of acoustic survey and commercial (October to December) length frequencies of sardine.

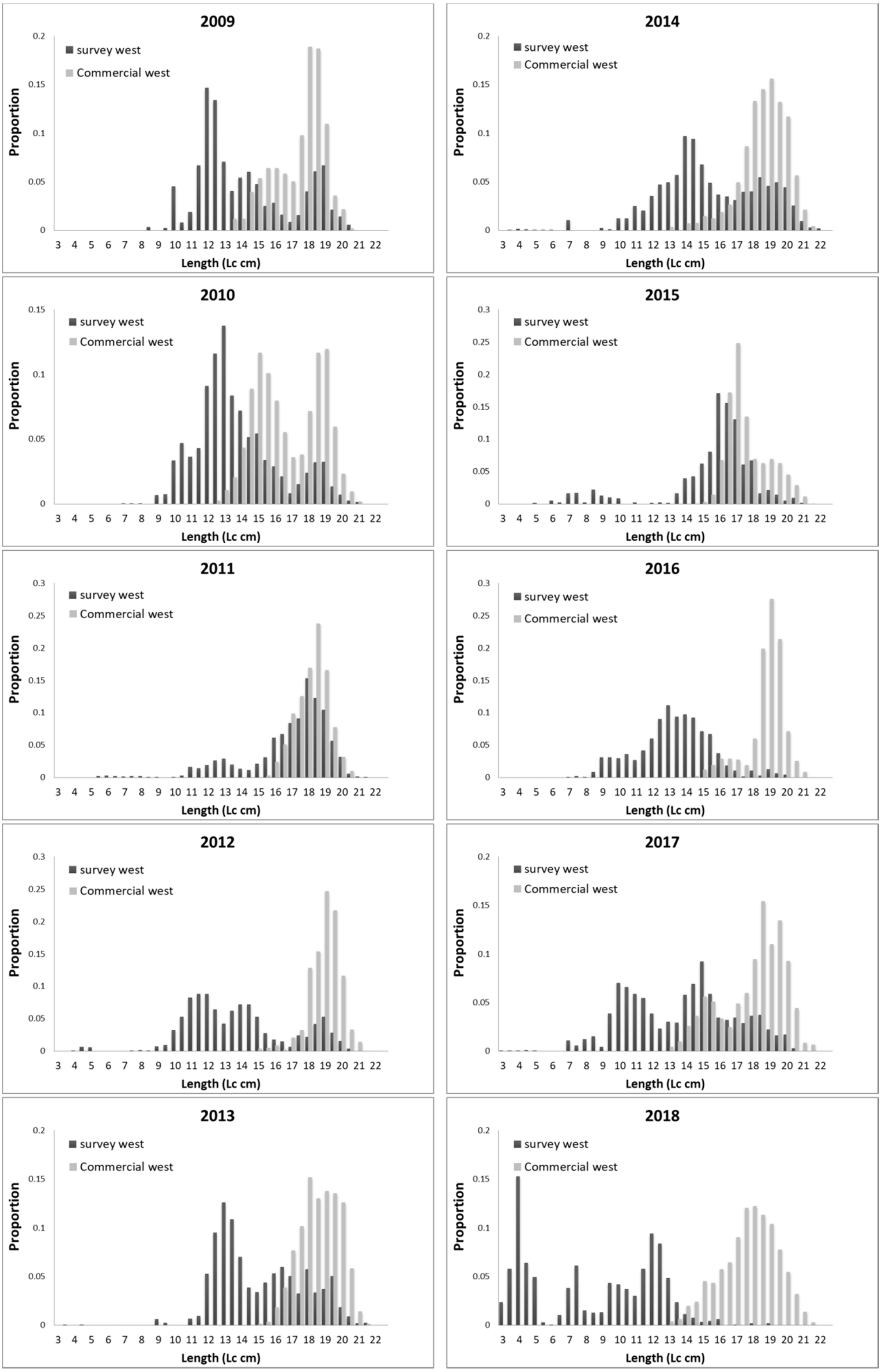

Figure B1. Sardine length frequencies from November surveys and commercial catches between October and November from 2009 to 2018 in the area to the west of Cape Agulhas.

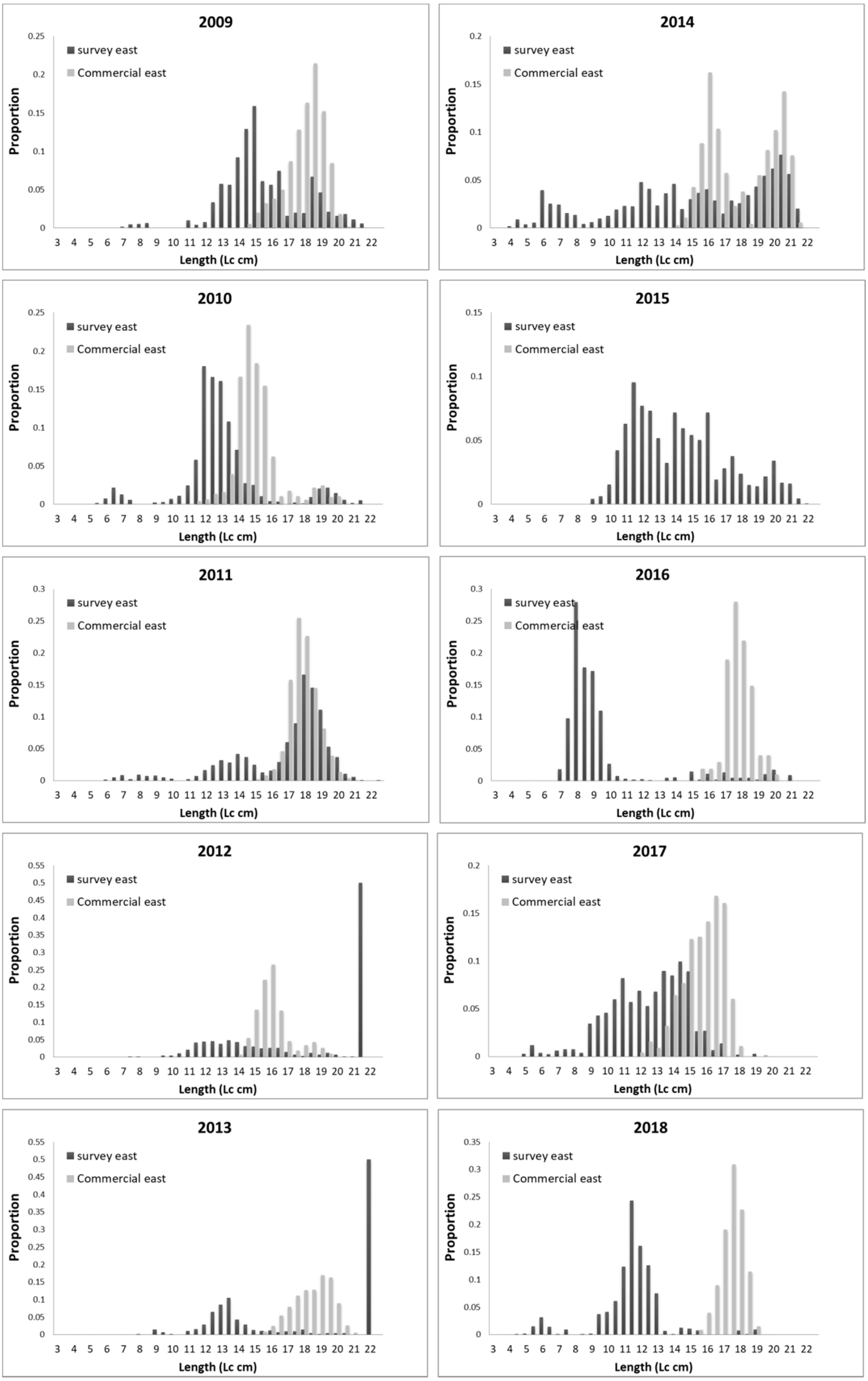

Figure B2. Sardine length frequencies from November surveys and commercial catches between October and November from 2009 to 2018 in the area to the east of Cape Agulhas.

Appendix C: Applying a regional (West Coast and South Coast) sardine length frequency at the interval level.

The impact on sardine and anchovy interval densities, biomass, CV and weighted length frequency of applying a “West Coast length frequency” for sardine to each trawl conducted on the West Coast and a “South Coast length frequency” for sardine to each trawl conducted on the South Coast is investigated. The original weighted by biomass length frequency of the November 2002 survey in the area to the west and east of Cape Agulhas is used as the West Coast and South Coast length frequency respectively. The sardine length frequency of each trawl used in the original calculation of sardine density is simply replaced by the appropriate regional length frequency. The original species composition is unchanged from that originally estimated for each trawl taken in the immediate vicinity.

Table C1. The impact on biomass of sardine and anchovy of applying a regional West Coast and South Coast length frequency at the interval level.

	Survey (tons)	CV	West Coast (tons)	CV	South Coast (tons)	CV
Original Sardine biomass	4 206 250	0.227	1 184 713	0.247	3 021 538	0.300
Modified sardine biomass	3 435 811	0.211	1 026 462	0.255	2 409 349	0.280
% change (-)	18.32		13.36		20.26	
Original anchovy biomass	3 867 649	0.154	2 018 570	0.264	1 849 079	0.144
Modified anchovy biomass	3 895 922	0.155	2 028 719	0.266	1 867 204	0.146
% change (+)	0.73		0.50		0.98	

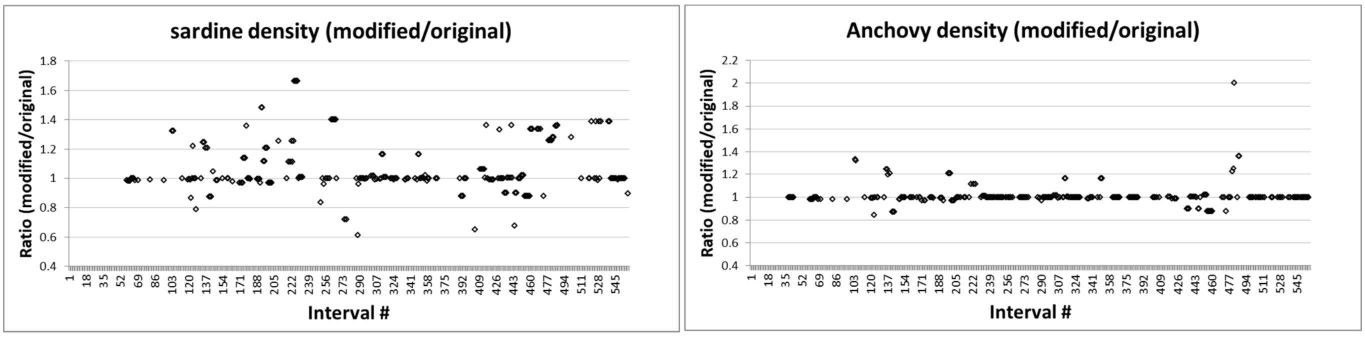

Figure C1. The ratio of the modified interval densities to the original interval densities for sardine (left) and anchovy (right).

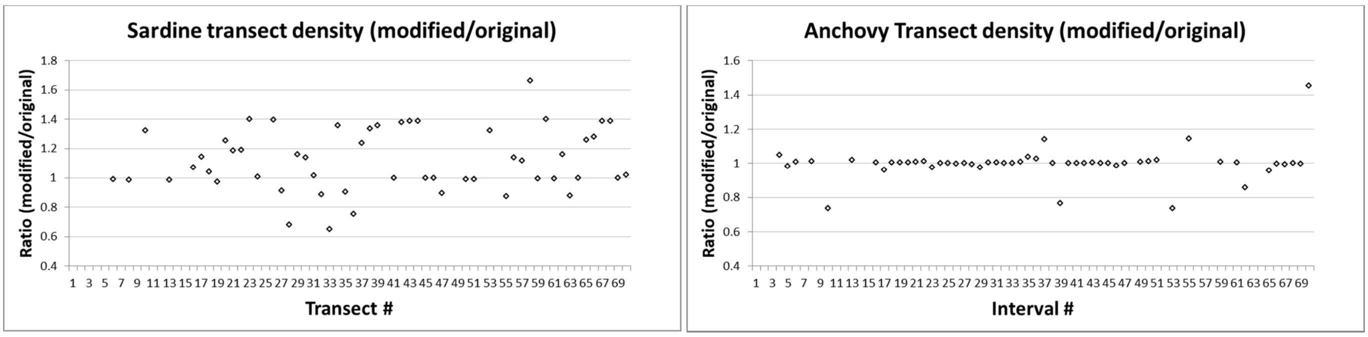

Figure C2. The ratio of the modified transect densities to the original transect densities for sardine (left) and anchovy (right).

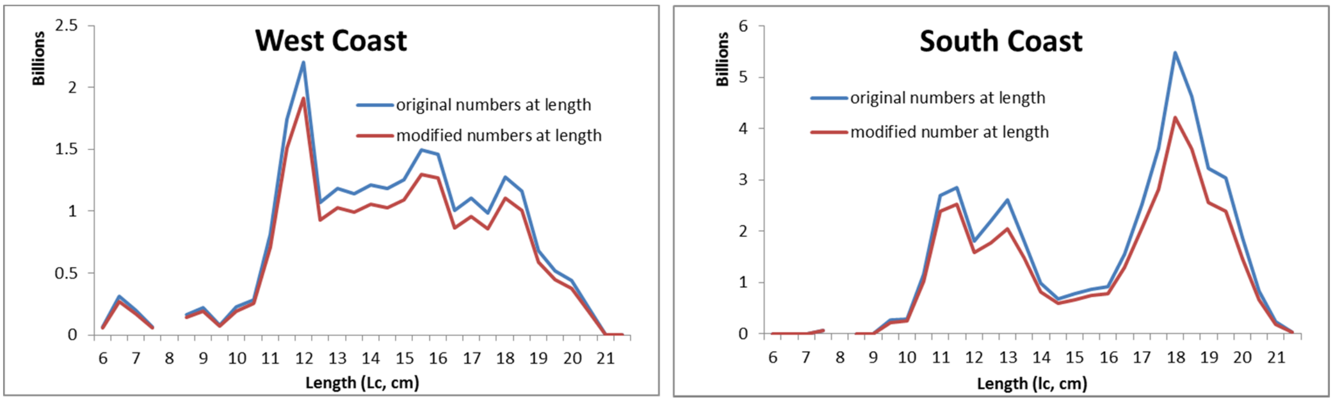

Figure C3. The original numbers at length (weighted by survey biomass) compared to that which would result from applying this regional length frequency to each trawl used in the calculation of sardine density for the West Coast (left) and South Coast (right).

Appendix D: Initial 2019 assessment model for the South African sardine resource (from de Moor 2019a,b)

This assessment provides the generalised operating model for the South African sardine resource (used for this baseline two mixing-component hypothesis as well as a single stock hypothesis[1]). The assessment is run from November $y_1 = 1984$ to November $y_n = 2018$, with the following subscript notation:

- quarters $q = 1$ denoting November $y-1$ to January y, $q = 2$ denoting February to April y, $q = 3$ denoting May to July y and $q = 4$ denoting August to October y;
- ages $a = 0$ to a plus group of $a = 5^+$;
- lengths from a minus group of $l = 2.5^- cm$ to a plus group of $l = 24^+ cm$;
- components $j = W$ or $j = S$ denote the west and south components, respectively, where only the west component equations are used in the single component hypothesis;
- infection $p = NI$ or $p = I$ denote the sardine uninfected and infected with the digenean 'tetracotyle-type' metacercarian endoparasite, respectively.

All parameters are defined in Tables D1 and D2.

Population Dynamics

Numbers-at-age at 1 November before movement or infection

$$N^{S*}_{j,p,y,a} = \left(\left(\left(\left(N^S_{j,p,y-1,a-1} e^{-M^S_{y,a-1}/8} - C^S_{j,p,y,1,a-1}\right) e^{-M^S_{y,a-1}/4} - C^S_{j,p,y,2,a-1}\right) e^{-M^S_{y,a-1}/4} - C^S_{j,p,y,3,a-1}\right) e^{-M^S_{y,a-1}/4} - C^S_{j,p,y,4,a-1}\right) e^{-M^S_{y,a-1}/8}$$

$$p = I, NI, y_1 \leq y \leq y_n, 1 \leq a \leq 4$$

$$N^{S*}_{j,p,y,5^+} = \left(\left(\left(\left(N^S_{j,p,y-1,4} e^{-M^S_{y,4}/8} - C^S_{j,p,y,1,4}\right) e^{-M^S_{y,4}/4} - C^S_{j,p,y,2,4}\right) e^{-M^S_{y,4}/4} - C^S_{j,p,y,3,4}\right) e^{-M^S_{y,4}/4} - C^S_{j,p,y,4,4}\right) e^{-M^S_{y,4}/8} +$$

$$\left(\left(\left(\left(N^S_{j,p,y-1,5^+} e^{-M^S_{y,5^+}/8} - C^S_{j,p,y,1,5^+}\right) e^{-M^S_{y,5^+}/4} - C^S_{j,p,y,2,5^+}\right) e^{-M^S_{y,5^+}/4} - C^S_{j,p,y,3,5^+}\right) e^{-M^S_{y,5^+}/4} - C^S_{j,p,y,4,5^+}\right) e^{-M^S_{y,5^+}/8}$$

$$p = I, NI, y_1 \leq y \leq y_n \qquad \text{(D1)}$$

Infection of west component sardine in the two mixing-component hypothesis; in the single component hypothesis $I_y = 0$ as the parasite data have no influence so that they are not included in the likelihood

$$\mathrm{N^{S**}_{W,NI,y,a}} = (1 - \mathrm{I_y})\mathrm{N^{S*}_{W,NI,y,a}} \qquad y_1 \leq y \leq y_n, 1 \leq a \leq 5^+$$

$$\mathrm{N^{S**}_{W,I,y,a}} = \mathrm{N^{S*}_{W,I,y,a}} + \mathrm{I_y N^{S*}_{W,NI,y,a}} \qquad y_1 \leq y \leq y_n, 1 \leq a \leq 5^+$$

$$\mathrm{N^{S**}_{S,p,y,a}} = \mathrm{N^{S*}_{S,p,y,a}} \qquad p = I, NI, y_1 \leq y \leq y_n, 1 \leq a \leq 5^+ \qquad \text{(D2)}$$

Movement of west component ($j = W$) sardine to the south component ($j = S$) in the two mixing-component hypothesis; in the single component hypothesis $move_{y,a} = 0$

$$\mathrm{N^{S}_{W,p,y,a}} = (1 - \mathrm{move_{y,a}})\mathrm{N^{S**}_{W,p,y,a}} \qquad p = I, NI, y_1 \leq y \leq y_n, 1 \leq a \leq 5^+$$

$$\mathrm{N^{S}_{S,p,y,a}} = \mathrm{N^{S**}_{S,p,y,a}} + \mathrm{move_{y,a} N^{S**}_{W,p,y,a}} \qquad p = I, NI, y_1 \leq y \leq y_n, 1 \leq a \leq 5^+ \qquad \text{(D3)}$$

[1] For the single stock hypothesis, both abundance indices and proportion-at-length data are combined for the full area and parasite prevalence-by-length is excluded from the likelihood.

Numbers-at-age mid-way through each quarter (for use in catch equations)

$N^S_{j,p,y,1,a} = N^S_{j,p,y-1,a} e^{-M^S_{y,a}/8}$ $\quad p = I, NI, y_1 \le y \le y_n, 0 \le a \le 5^+$

$N^S_{j,p,y,q,a} = \left(N^S_{j,p,y,q-1,a} - C^S_{j,p,y,q-1}\right) e^{-M^S_{y,a}/4}$ $\quad p = I, NI, y_1 \le y \le y_n, 2 \le q \le 4, 0 \le a \le 5^+$ (D4)

Numbers-at-length at 1 November (after infection and movement)

The model estimated numbers-at-length range from a 2.5cm minus group to a 24cm plus group, denoted 2.5^- and 24^+, respectively, in the remaining text.

$N^S_{j,p,y,l} = \sum_{a=0}^{5^+} A^{sur}_{j,y,a,l} N^S_{j,p,y,a}$ $\quad p = I, NI, y_1 \le y \le y_n, 2.5^- cm \le l \le 24^+ cm$ (D5)

The model predicted numbers-at-length of ages 1+ only are given by:

$N^{S,1+}_{j,p,y,l} = \sum_{a=1}^{5^+} A^{sur}_{j,y,a,l} N^S_{j,p,y,a}$ $\quad p = I, NI, y_1 \le y \le y_n, 2.5^- cm \le l \le 24^+ cm$ (D6)

The proportion of sardine of age a in component j that fall in length group l at 1 November, $A^{sur}_{j,y,a,l}$, is calculated under the assumption that length-at-age is normally distributed about a von Bertalanffy growth curve:

$A^{sur}_{j,y,a,l} \sim N\left(L_{j,\infty}\left(1 - e^{-\kappa_j(a - t_{0,j,y-a})}\right), \vartheta_a^2\right)$ [2] $\quad y_1 \le y \le y_n, 0 \le a \le 5^+, 2.5^- cm \le l \le 24^+ cm$ (D7)

with

$t_{0,j,y} = t_{0,j} + \varepsilon^t_y$ [3] (D8)

And $\varepsilon^t_y = \begin{cases} \eta^t_y & y = y_1 \\ \rho^t \varepsilon^t_{y-1} + \sqrt{1 - (\rho^t)^2}\,\eta^t_y & y_1 < y \le y_n \end{cases}$

Natural mortality

Natural mortality is modelled to vary annually in an autocorrelated manner around a median as follows (although the baseline assumes no such correlation – see Table A.1):

$M^S_{y,a=0} = \bar{M}^S_{ju} e^{\varepsilon^{ju}_y}$ with $\varepsilon^{ju}_{1984} = \eta^{ju}_{1984}$ and $\varepsilon^{ju}_y = \rho \varepsilon^{ju}_{y-1} + \sqrt{1 - \rho^2}\,\eta^{ju}_y$, $y_1 \le y \le y_n$ (D9)

$M^S_{y,a=1+} = \bar{M}^S_{ad} e^{\varepsilon^{ad}_y}$ with $\varepsilon^{ad}_{1984} = \eta^{ad}_{1984}$ and $\varepsilon^{ad}_y = \rho \varepsilon^{ad}_{y-1} + \sqrt{1 - \rho^2}\,\eta^{ad}_y$, $y_1 \le y \le y_n$ (D10)

Spawning biomass and biomass associated with the November survey

$SSB^S_{j,y} = \sum_p \sum_{l=2.5^-}^{24^+} f^S_{j,y,l} N^{S,1+}_{j,p,y,;} w^S_{j,l}$ $\quad y_1 \le y \le y_n$ (D11)

$SSB^{eff,S}_{j=W,y} = \xi_W SSB^S_{W,y} + (1 - \xi_S) SSB^S_{S,y}$ $\quad y_1 \le y \le y_n$

$SSB^{eff,S}_{j=S,y} = (1 - \xi_W) SSB^S_{W,y} + \xi_S SSB^S_{S,y}$ $\quad y_1 \le y \le y_n$ (D12)

$B^S_{j,y} = k^S_{j,N} \sum_p \sum_{l=2.5^-}^{24^+} N^S_{j,p,y,l} w^S_{j,l}$ [4,5] $\quad y_1 \le y \le y_n$ (D13)

---

[2] Given the allowance for early/late recruitment in varying $t_{0,y}$ estimates annually, there may be some proportion of this distribution below a length of zero (due to late recruitment). In these cases, this proportion is removed from the proportion-at-length of the minus length class.

[3] Additive error allows for early or late recruitment. While the timing of recruitment may vary between stocks due to differing environmental conditions on the west and south coasts, the same autocorrelation parameters are assumed here for simplicity reasons.

[4] The biomass in $y_n = 2018$ excludes age 0 fish, although the contribution of age 0 fish to the total biomass should be minor.

[5] A time invariant weight-at-length is used in this equation. Previous assessments adjusted the November weight-at-length annually, informed by the average weight of sardine sampled during the survey, to account for the differing condition factor of sardine at the time of the survey. However, recent discussions have clarified that the hydro-acoustic survey estimate of total biomass depends on the size of the fish swim bladder which depends (through the time invariant target strength relationship) on fish length only but not on the condition (skinniness/fattiness) of the fish at the time of the survey. A time-invariant weight-at-length therefore provides most

Commercial selectivity

$$S_{j,y,q,l} = \begin{cases} 0 & l \leq 5.5cm \\ \chi_{j,y,q} exp\left\{-\frac{\left(l+0.25-\bar{l}_{1,y}\right)^2}{(\sigma_1^{sel})^2}\right\} + \frac{1}{1+exp\left\{-\left(l+0.25-\bar{l}_{2,j,y,q}\right)/(\sigma_2^{sel})^2\right\}} & 6cm \leq l \leq l_{max} = 23cm \\ S_{j,y,q,lmax} & l > l_{max} \end{cases}$$ [6]

$$y_1 \leq y \leq y_n,\ 1 \leq q \leq 4 \quad \text{(D14)}$$

$$S_{j,y,q,a} = \sum_{l=2.5^-}^{24^+} A_{j,y,q,a,l}^{com} S_{j,y,q,l} \qquad y_1 \leq y \leq y_n,\ 1 \leq q \leq 4,\ 0 \leq a \leq 5^+ \quad \text{(D15)}$$

where $A_{j,y,q,a,l}^{com} \sim N\left(L_{j,\infty}\left(1-e^{-\kappa_j\left(a+(2q-1)/8-t_{0,j,y-a}\right)}\right), \left[\left(1-\frac{(2q-1)}{8}\right)\vartheta_a + \frac{(2q-1)}{8}\vartheta_{a+1}\right]^2\right)$

$$y_1 \leq y \leq y_n,\ 1 \leq q \leq 4, 0 \leq a \leq 5^+,\ 2.5^- cm \leq l \leq 24^+ cm \quad \text{(D16)}$$

Bycatch in the anchovy directed fishery

$$C_{j,p,y,q,a}^{bycatch} = \begin{cases} N_{j,p,y,q,a}^S F_{j,y,q,a}^{By} & 0 \leq a \leq 1 \\ 0 & 2 \leq a \leq 5^+ \end{cases} \qquad p = I, NI, y_1 \leq y \leq y_n,\ 1 \leq q \leq 4 \quad \text{(D17)}$$ [7]

Catch in the directed sardine and round herring bycatch fisheries

$$C_{j,p,y,q,a}^{dir} = \left(N_{j,p,y,q,a}^S - C_{j,p,y,q,a}^{bycatch}\right) S_{j,y,q,a} F_{j,y,q} \qquad p = I, NI, y_1 \leq y \leq y_n,\ 1 \leq q \leq 4, 0 \leq a \leq 5^+ \quad \text{(D18)}$$

Total catch

$$C_{j,p,y,q,a}^S = C_{j,p,y,q,a}^{bycatch} + C_{j,p,y,q,a}^{dir} \qquad p = I, NI, y_1 \leq y \leq y_n,\ 1 \leq q \leq 4, 0 \leq a \leq 5^+ \quad \text{(D19)}$$

Fished proportion of the available biomass from the sardine bycatch with the anchovy directed fishery

$$F_{j,y,q=1,a=0}^{By} = \frac{\sum_{m=11}^{12} \sum_{l<lcut_{y-1,m}} C_{j,y-1,m,l}^{RLF,fleet=3} + \sum_{l<lcut_{y,m}} C_{j,y,1,l}^{RLF,fleet=3}}{\sum_p N_{j,p,y,q=1,a=0}^S}$$

$$F_{j,y,q=1,a=1}^{By} = \frac{\sum_{m=11}^{12} \sum_{l\geq lcut_{y-1,m}} C_{j,y-1,m,l}^{RLF,fleet=3} + \sum_{l\geq lcut_{y,m}} C_{j,y,1,l}^{RLF,fleet=3}}{\sum_p N_{j,p,y,q=4,a=1}^S}$$

$$F_{j,y,q=2,a=0}^{By} = \frac{\sum_{m=2}^{4} \sum_{l<lcut_{y,m}} C_{j,y,m,l}^{RLF,fleet=3}}{\sum_p N_{j,p,y,q=2,a=0}^S} \qquad F_{j,y,q=2,a=1}^{By} = \frac{\sum_{m=2}^{4} \sum_{l\geq lcut_{y,m}} C_{j,y,m,l}^{RLF,fleet=3}}{\sum_p N_{j,p,y,q=2,a=1}^S}$$

$$F_{j,y,q=3,a=0}^{By} = \frac{\sum_{m=5}^{7} \sum_{l<lcut_{y,m}} C_{j,y,m,l}^{RLF,fleet=3}}{\sum_p N_{j,p,y,q=3,a=0}^S} \qquad F_{j,y,q=3,a=1}^{By} = \frac{\sum_{m=5}^{7} \sum_{l\geq lcut_{y,m}} C_{j,y,m,l}^{RLF,fleet=3}}{\sum_p N_{j,p,y,q=3,a=1}^S}$$

$$F_{j,y,q=4,a=0}^{By} = \frac{\sum_{m=8}^{10} \sum_{l<lcut_{y,m}} C_{j,y,m,l}^{RLF,fleet=3}}{\sum_p N_{j,p,y,q=4,a=0}^S} \qquad F_{j,y,q=4,a=1}^{By} = \frac{\sum_{m=8}^{10} \sum_{l\geq lcut_{y,m}} C_{j,y,m,l}^{RLF,fleet=3}}{\sum_p N_{j,p,y,q=4,a=1}^S} \quad \text{(D20)}$$

A penalty is imposed within the model to ensure that $F_{j,y,q,a}^{By} < 0.95$.

Fished proportion of the available biomass from the directed sardine catch and sardine bycatch with round herring fishery

---

appropriate basis to estimate biomass from the population model to correspond to the time series of biomasses from the survey (which is independent of sardine condition factor).

[6] The $l + 0.25$ denotes the middle of length class l. This function is renormalized to a maximum of 1.

[7] "Selectivity" is incorporated in $F_{j,y,q,a}^{By}$, as the sardine bycaught is typically independent of sardine abundance, but rather correlated with anchovy recruitment which varies from year to year.

$$F_{j,y,q=1} = \frac{\sum_{fleet=1}^{2}\sum_{m=11}^{12}\sum_{l\geq 6cm} C_{j,y-1,m,l}^{RLF,fleet} + \sum_{fleet=1}^{2}\sum_{l\geq 6cm} C_{j,y,1,l}^{RLF,fleet}}{\sum_p \sum_{a=0}^{5+}\left(N_{j,p,y,1,a}^S - C_{j,y,1,a}^{bycatch}\right) S_{j,y,1,a}}$$

$$F_{j,y,q=2} = \frac{\sum_{fleet=1}^{2}\sum_{m=2}^{4}\sum_{l\geq 6cm} C_{j,y,m,l}^{RLF,fleet}}{\sum_p \sum_{a=0}^{5+}\left(N_{j,p,y,2,a}^S - C_{j,y,2,a}^{bycatch}\right) S_{j,y,2,a}}$$

$$F_{j,y,q=3} = \frac{\sum_{fleet=1}^{2}\sum_{m=5}^{7}\sum_{l\geq 6cm} C_{j,y,m,l}^{RLF,fleet}}{\sum_p \sum_{a=0}^{5+}\left(N_{j,p,y,3,a}^S - C_{j,y,3,a}^{bycatch}\right) S_{j,y,3,a}}$$

$$F_{j,y,q=4} = \frac{\sum_{fleet=1}^{2}\sum_{m=8}^{10}\sum_{l\geq 6cm} C_{j,y,m,l}^{RLF,fleet}}{\sum_p \sum_{a=0}^{5+}\left(N_{j,p,y,4,a}^S - C_{j,y,4,a}^{bycatch}\right) S_{j,y,4,a}} \qquad \text{(D21)}$$

A penalty is imposed within the model to ensure that $S_{j,y,a,l}F_{j,y,q} < 0.95$. Fish <6cm were seldom[8] caught and were thus not used in fitting this model. Commercial selectivity-at-length is fixed to zero for length classes <6cm (equation D12).

Number of recruits associated with the recruit survey

$$N_{j,y,r}^S = k_{j,r}^S \left(\left(N_{j,NI,y,2,0}^S - C_{j,NI,y,2,0}^S\right) e^{-(1/8+0.5t_y^S/12)M_{y,0}^S} - \tilde{C}_{j,y,0bs}^S \right) e^{-0.5t_y^S \times M_{y,0}^S/12} \quad 1985 \leq y \leq y_n \qquad \text{(D22)}$$

Multiplicative survey bias

$$k_{j,N}^S = k_{ac}^S \qquad \text{(D23)}$$

$$k_{j=W,r}^S = k_{cov}^S \times k_{ac}^S \qquad \text{(D24)}$$

$k_{j=S,r}^S = k_{covS}^S \times k_{cov}^S \times k_{ac}^S$ (for the two mixing-component hypothesis only) (D25)

Survey trawl selectivity

$$S_{j,l}^{survey} = \begin{cases} 0 & l = 2.5^- cm \\ \left[1 + exp\left\{-\left(l + 0.25 - S_{50,j}\right)/\delta_j\right\}\right]^{-1} & 3cm \leq l \leq 24^+ cm \end{cases} \qquad y_1 \leq y \leq y_n \text{(D26)}$$

Proportion-at-length associated with the November survey

$$p_{j,y,l}^S = \begin{cases} \frac{\sum_p \sum_{l\leq 6cm} N_{j,p,y,l}^S S_{j,l}^{survey}}{\sum_p \sum_{l=2.5^-}^{24^+} N_{j,p,y,l}^S S_{j,l}^{survey}} & l = 6^- cm \\ \frac{\sum_p N_{j,p,y,l}^S S_{j,l}^{survey}}{\sum_p \sum_{l=2.5^-}^{24^+} N_{j,p,y,l}^S S_{j,l}^{survey}} & 6.5cm \leq l \leq 20.5cm \\ \frac{\sum_p \sum_{l=21}^{23.5} N_{j,p,y,l}^S S_{j,l}^{survey}}{\sum_p \sum_{l=2.5^-}^{24^+} N_{j,p,y,l}^S S_{j,l}^{survey}} & l = 21 - 23.5cm \\ \frac{\sum_p N_{j,p,y,l}^S S_{j,24^+}^{survey}}{\sum_p \sum_{l=2.5^-}^{24^+} N_{j,p,y,l}^S S_{j,l}^{survey}} & l = 24^+ cm \end{cases} \text{[9]} \qquad y_1 \leq y \leq y_n \qquad \text{(D27)}$$

Proportion-at-length of fish infected with the parasite in November

$$P_{j,y,l}^S = \frac{N_{j,I,y,l}^S}{\sum_p N_{j,p,y,l}^S} \qquad y_1 \leq y \leq y_n, 10cm \leq l \leq 23cm \qquad \text{(D28)}$$

Catch-at-length from the directed and round herring bycatch fisheries

[8] Less than 6% of the quarters west of Cape Agulhas, less than 2% of the quarters south-east of Cape Agulhas and less than 4% of the quarters for the whole coast.

[9] The inclusion of model predicted proportion-at-length 24$^+$cm is deliberate to take into account the zero samples of 24$^+$cm sardine in the survey.

$C^{dir}_{j,p,y,q,l} = \sum_{a=0}^{5^+}\left(N^S_{j,p,y,q,a} - C^{bycatch}_{j,p,y,q,a}\right)A^{com}_{j,q,a,l}S_{j,y,q,l}F_{j,y,q}$ [10]

$$p = I, NI, y_1 \le y \le y_n,\ 1 \le q \le 4,\ 2.5^- cm \le l \le 24^+ cm \quad \text{(D29)}$$

Proportion-at-length associated with the directed catch and round herring bycatch

$$p^{coml,S}_{j,y,q,l} = \begin{cases} \dfrac{\sum_p C^{dir}_{j,p,y,q,l}}{\sum_p \sum_{l=6}^{24^+} C^{dir}_{j,p,y,q,l}} & 6cm \le l \le 22.5cm \\ \dfrac{\sum_p \sum_{l=23}^{24^+} C^{dir}_{j,p,y,q,l}}{\sum_p \sum_{l=6}^{24^+} C^{dir}_{j,p,y,q,l}} & l = 23^+ cm \end{cases} \quad [11] \quad y_1 \le y \le y_n,\ 1 \le q \le 4 \quad \text{(D30)}$$

<u>Fitting the Model to Observed Data (Likelihood)</u>

$$-lnL = -lnL^{Nov} - lnL^{rec} - lnL^{sur\ propl} - lnL^{com\ propl} - lnL^{prev} \quad \text{(D31)}$$

where

$$-lnL^{Nov} = 0.5\sum_j \sum_{y=y_1}^{y_n} \left\{ \frac{5^5\left(\frac{\left|ln\left(\hat{B}^S_{j,y}\right) - ln\left(B^S_{j,y}\right)\right|}{\sqrt{\left(\sigma^S_{j,y,Nov}\right)^2 + \left(\phi^S_{ac}\right)^2 + \left(\lambda^S_{j,N}\right)^2}}\right)^5}{5^5 + \left(\frac{\left|ln\left(\hat{B}^S_{j,y}\right) - ln\left(B^S_{j,y}\right)\right|}{\sqrt{\left(\sigma^S_{j,y,Nov}\right)^2 + \left(\phi^S_{ac}\right)^2 + \left(\lambda^S_{j,N}\right)^2}}\right)^5} \right\}^{2/5} + ln\left[2\pi\left(\left(\sigma^S_{j,y,Nov}\right)^2 + (\phi^S_{ac})^2 + \left(\lambda^S_{j,N}\right)^2\right)\right] \quad \text{(D32)}$$

$$-lnL^{rec} = 0.5\sum_j \sum_{y=y_2}^{y_n} \left\{ \frac{5^5\left(\frac{\left|ln\left(\hat{N}^S_{j,y,r}\right) - ln\left(N^S_{j,y,r}\right)\right|}{\sqrt{\left(\sigma^S_{j,y,rec}\right)^2 + \left(\phi^S_{ac}\right)^2 + \left(\lambda^S_{j,r}\right)^2}}\right)^5}{5^5 + \left(\frac{\left|ln\left(\hat{N}^S_{j,y,r}\right) - ln\left(N^S_{j,y,r}\right)\right|}{\sqrt{\left(\sigma^S_{j,y,rec}\right)^2 + \left(\phi^S_{ac}\right)^2 + \left(\lambda^S_{j,r}\right)^2}}\right)^5} \right\}^{2/5} + ln\left[2\pi\left(\left(\sigma^S_{j,y,rec}\right)^2 + (\phi^S_{ac})^2 + \left(\lambda^S_{j,r}\right)^2\right)\right] \quad \text{(D33)}$$

$$-lnL^{sur\ propl} = w^{sur}_{propl}\sum_j \sum_{y=y_1}^{y_n} \left\{ \sum_{l=6^-}^{21^+} \left\{ \frac{\left(\sqrt{\hat{p}^S_{j,y,l}} - \sqrt{p^S_{j,y,l}}\right)^2}{2\left(\sigma^S_{j,sur}\right)^2} + ln\left(\sigma^S_{j,sur}\right) \right\} + \frac{\left(0 - \sqrt{p^S_{j,y,24^+}}\right)^2}{2\left(\sigma^S_{j,sur}\right)^2} + ln\left(\sigma^S_{j,sur}\right) \right\} \quad [12] \quad \text{(D34)}$$

$$-lnL^{com\ propl} = w^{com}_{propl}\sum_j \sum_{y=y_1}^{y_n} \sum_{q=1}^{4} \sum_{l=6}^{23^+} \left\{ \frac{\left(\sqrt{\hat{p}^{S,coml}_{j,y,q,l}} - \sqrt{p^{S,coml}_{j,y,q,l}}\right)^2}{2\left(\sigma^S_{j,com}\right)^2} + ln\left(\sigma^S_{j,com}\right) \right\} \quad \text{(D35)}$$

$$-lnL^{prev} = \sum_j \sum_{y=2010}^{2018} \sum_{l=10cm}^{23cm} -n^{prev}_{j,y,l}\, ln\left(P^S_{j,y,l}\right) - \left(N^{prev}_{j,y,l} - n^{prev}_{j,y,l}\right) ln\left(1 - P^S_{j,y,l}\right) \quad \text{(D36)}$$

A "robustified likelihood" is used for the contributions from the hydro-acoustic surveys to ensure no undue influence from any extreme (outlying) values for residuals. The functional form chosen to robustify makes negligible difference for standardised residuals of magnitude three or less, but essentially treats large standardised residuals as if they do not exceed five in magnitude.

[10] Note the model predicted commercial catch of lengths <6cm is zero, from a zero commercial selectivity in equation A.13. This is consistent with the range of length classes in the observed commercial proportions-at-lengths.

[11] Note the model predicted commercial catch of lengths <6cm is zero, from a zero commercial selectivity in equation A.13. This is consistent with the range of length classes in the observed commercial proportions-at-lengths.

[12] The 21^+ group in this equation consists of the length classes 21cm, 21.5cm, 22cm, 22.5cm, 23cm and 23.5cm.

Table D1. Assessment model parameters and variables with associated fixed values or prior distributions and, for derived variables, associated equation numbers. As the majority of prior distributions are uninformative, notes are provided only for informative priors and/or bounds.

	Parameter / Variable	Description	Units / Scale	Fixed Value / Prior Distribution	Equation	Notes
Annual numbers and biomass	$N^S_{j,p,y,a}$	Model predicted numbers-at-age a at the beginning of November in year y of component j that are uninfected ($p = NI$) or infected ($p = I$) with the endoparasite	Billions	$ln(N^S_{j,NI,y,0})/10 \sim U(-10,3.$ $N^S_{j,I,y,0} = 0$	D1 - D3	
	$N^S_{j,p,1983,a}$	Initial numbers-at-age a in component j	Billions	$N^S_{j,NI,1983,a=1} \sim U(0,50)$ $N^S_{j,NI,1983,a} = 0,\ 2 \le a \le 5^+$ $N^S_{j,I,1983,a} = 0,\ 0 \le a \le 5^+$		
	$N^S_{j,p,y,q,a}$	Model predicted numbers-at-age a mid-way through quarter q of year y of component j that are uninfected ($p = NI$) or infected ($p = I$) with the endoparasite	Billions		D4	
	I_y	Proportion of uninfected west component sardine that are infected with the endoparasite in year y (two mixing-component hypothesis only)		$= 0,\ y_1 \le y \le 2007$ $\sim U(0,1),\ 2008 \le y \le y_n$		
	$move_{y,a}$	Proportion of west component sardine of age a which move to the south component at the beginning of November of year y (two mixing-component hypothesis only)	-	$move_{y,1} \sim Beta(1.05,1.05)$ $move_{y,2+} = \phi move_{y,1}$ $\phi \sim U(0,1)$		
	$SSB^S_{j,y}$	Model predicted spawning biomass of component j at the beginning of November in year y	Thousand tons		D11	
	$SSB^{eff,S}_{j,y}$	Model predicted effective spawning biomass of component j at the beginning of November in year y	Thousand tons		D12	
	$B^S_{j,y}$	Model predicted total biomass of component j at the beginning of November in year y, associated with the November survey	Thousand tons		D13	
	ξ_j	Proportion of j-component spawner biomass that contributes to the effective spawning biomass on the same coast		0.08		Alternative values considered in robustness tests
	$w^S_{j,l}$	Mean mass of sardine of component j in length class l	Grams	$1.1639 \times 10^{-5} \times l^{3.03155}$		van der Lingen *et al.* (2006)

Table D1 (Continued).

	Parameter / Variable	Description	Units / Scale	Fixed Value / Prior Distribution	Equation	Notes
Annual numbers and biomass	$f_{j,y,l}^{S}$	Proportion of component j sardine that are mature in length class l in year y	-	$\left[1+e^{-(l-17.2)/1.17}\right]^{-1}$ $1984 \le y \le 1987$ $\left[1+e^{-(l-18.6)/1.26}\right]^{-1}$ $1988 \le y \le 1995$ $\left[1+e^{-(l-19.4)/1.40}\right]^{-1}$ $1996 \le y \le 2003$ $\left[1+e^{-(l-17.4)/0.95}\right]^{-1}$ $2004 \le y \le 2018$		Refit from data used by van der Lingen *et al*. (2006) using midpoints of length classes. Assuming maturity post-2003 reflects that of 1965-1975 as maturity is hypothesized to be density dependent (van der Lingen *et al*. 2006) and both these periods correspond to low biomass following a peak in abundance
	$N_{j,y,r}^{S}$	Model predicted number of juveniles of component j at the time of the recruit survey in year y	Billions		D23	
Natural mortality	$M_{y,a}^{S}$	Rate of natural mortality of age a in year y	Year^{-1}	$M_{y,0}^{S}=1.0$ $M_{y,1+}^{S}=1.0$	D9 and D10	Selected based on maximized joint posterior, and subject to a compelling reason to modify from previous assessment
	$\bar{M}_{ju}^{S}$	Median juvenile rate of natural mortality	Year^{-1}	1.0		
	$\bar{M}_{ad}^{S}$	Median rate of natural mortality for 1+ sardine	Year^{-1}	0.8		
	ε_{y}^{ju}	Annual residuals about juvenile natural mortality rate	-		D9	
	ε_{y}^{ad}	Annual residuals about natural mortality rate for 1+ sardine	-		D10	
	η_{y}^{ju}	Normally distributed error in calculating ε_{y}^{ju}	-	$N\left(0,\sigma_{j}^{2}\right)$		
	η_{y}^{ad}	Normally distributed error in calculating ε_{y}^{ad}	-	$N(0,\sigma_{ad}^{2})$		
	σ_{j}	Standard deviation in the annual residuals about juvenile natural mortality	-	0		See robustness tests
	σ_{ad}	Standard deviation in the annual residuals about natural mortality for ages 1+	-	0		See robustness tests
	ρ	Annual autocorrelation coefficient	-	0		See robustness tests

Table D1 (Continued).

	Parameter / Variable	Description	Units / Scale	Fixed Value / Prior Distribution	Equation	Notes
Proportions-at-length and growth curve	$N^{S}_{j,p,y,l}$	Model predicted numbers-at-length l at the beginning of November in year y of component j that are uninfected ($p = NI$) or infected ($p = I$) with the endoparasite	Billions		D5	
	$p^{S}_{j,y,l}$	Model predicted proportion-at-length l of component j associated with the November survey in year y	-		D27	
	$A^{sur}_{j,y,a,l}$	Proportion of age a of component j sardine that falls in the length group l in November of year y	-		D7	
	κ_j	Somatic growth rate parameter for component j	Year^{-1}	$U(0,3)$		
	$L_{j,\infty}$	Maximum length (in expectation) of component j	Cm	$L_{j,\infty} = \frac{L_{j,1}e^{-2\kappa_j}-L_{j,3}}{e^{-2\kappa_j}-1}$ where $L_{j,a=1} \sim U(5,25)$ $L_{j,a=3} - L_{j,a=1} \sim U(5,25)$		
	$t_{0,j,y}$	Age at which the length (in expectation) is zero in year y	Year		D8	
	$t_{0,j}$	Average age at which the length (in expectation) is zero	Year	$\frac{1}{\kappa_j} ln \left\{ \frac{e^{\kappa_j}(L_{j,1} - L_{j,3})}{L_{j,1}e^{-2\kappa_j} - L_{j,3}} \right\}$		
	ε^{t}_{y}	Annual residuals about the age at which the length is zero		$\eta^{t}_{y} \sim N(0, 0.2^2)$		
	ρ^{t}	Autocorrelation coefficient in these residuals		$U(-1,1)$		
	ϑ_a	Standard deviation of the distribution about the mean length for age a	-	$U(0,3)$, $a = 0,1,2^{+}$		Upper bound chosen to preclude unrealistically large lengths for very young fish
	$p^{com,S}_{j,y,q,l}$	Model predicted proportion-at-length l of component j in the directed catch and round herring bycatch during quarter q of year y	-		D30	
	$A^{com}_{j,y,q,a,l}$	Proportion of age a of component j sardine that falls in the length group l mid-way through quarter q of year y	-		D16	
	$P^{S}_{j,y,l}$	Model predicted proportion-at-length l of component j that are infected with the endoparasite, at the time of the November survey in year y			D28	

Table D1 (Continued).

	Parameter / Variable	Description	Units / Scale	Fixed Value / Prior Distribution	Equation	Notes
Selectivity	$S_{j,l}^{survey}$	Survey selectivity-at-length l in the November survey for component j	-		D26	Some smaller fish escape through the trawl net
	$S_{50,j}$	Length at which survey selectivity is 50% for component j	Cm	$U(2.5{,}20)$		
	δ_j	Inverse of slope of survey selectivity-at-length ogive when selectivity is 50% for component j	-	$U(0.05{,}50)$		
	$S_{j,y,q,l}$	Commercial selectivity-at-length l during quarter q of year y of component j	-		D14	
	$S_{j,y,q,a}$	Commercial selectivity-at-age a during quarter q of year y of component j	-		D15	
	$\chi_{j,y,q}$	Height of the Gaussian component for component j relative to the height of the logistic component in quarter q of year y	-	$U(0{,}1)$ for $j=1$ = 0 for $j=2$		No bycatch modelled for south component
	$\bar{l}_{1,y}$	Mean of the Gaussian distribution for in year y	mm	$N(100, 10^2)$		
	$\bar{l}_{2,j,y,q}$	Length at 50% selectivity in the logistic component for component j in quarter q of year y	mm	$\bar{l}_{2,j,y,1} - \bar{l}_{1,2000} \sim U(0{,}150)$ $\bar{l}_{2,j,y,2} - \bar{l}_{1,2000} \sim U(0{,}150)$ $\bar{l}_{2,j,y,3} = \bar{l}_{2,j,y,2}$ $\bar{l}_{2,j,y-1,4} = \bar{l}_{2,j,y12}$		Estimated for two time periods per component: 1984-1993, 1994-2018 (west) and 1984-1997, 1998-2018 (south)
	$(\sigma_1^{sel})^2$	Variance parameter of the Gaussian distribution	mm	$U(20{,}150)$		
	$(\sigma_2^{sel})^2$	Variance parameter of the logistic distribution	mm	$U(0{,}100)$		
Multiplicative bias	$k_{j,N}^S$	Multiplicative bias associated with the November survey of component j	-		D23	
	$k_{j,r}^S$	Multiplicative bias associated with the recruit survey of component j	-		D24 – D25	
	k_{ac}^S	Multiplicative bias associated with the hydro-acoustic survey	-	$ln(k_{ac}^S) \sim N(-0.311, 0.094^2)$		Appendix B of de Moor and Butterworth (2016)
	k_{cov}^S	Multiplicative bias associated with the coverage of the recruits during the recruit survey in comparison to the coverage of the biomass during the November survey	-	Uniform prior on logit transpose of k_{cov}^S, such that $0.3 \leq k_{cov}^S \leq 1$		Lower bound selected in discussions with scientists on these surveys and their field experience
	k_{covS}^S	Multiplicative bias associated with the coverage of the south component recruits in comparison to the west component recruits during the recruit survey		$U(0{,}1)$		

Table D1 (Continued).

	Parameter / Variable	Description	Units / Scale	Fixed Value / Prior Distribution	Equation	Notes
Catch	$C^{S}_{j,p,y,q,a}$	Model predicted number of age a fish of component j caught during quarter q of year y that are uninfected ($p = NI$) or infected ($p = I$) with the endoparasite	Billions		D19	
	$lcut_{y,m}$	Cut off length for recruits in month m of year y	Cm	de Moor *et al*. 2019		Differ by month and year as informed by the recruit surveys
	$C^{bycatch}_{j,p,y,q,a}$	Number of age a fish of component j bycaught in the anchovy-directed fishery in quarter q of year y that are uninfected ($p = NI$) or infected ($p = I$) with the endoparasite	Billions		D17	
	$C^{dir}_{j,p,y,q,a}$	Number of age a fish of component j caught in the sardine-directed and round herring bycatch fisheries in quarter q of year y that are uninfected ($p = NI$) or infected ($p = I$) with the endoparasite	Billions		D18	
	$C^{dir}_{j,p,y,q,l}$	Number of length l fish of component j caught in the sardine-directed and round herring bycatch fisheries in quarter q of year y	Billions		D29	
	$F^{By}_{j,y,q,a}$	Fished proportion in quarter q of year y for age class a of component j, of bycatch in the anchovy-directed fishery	-		D20	
	$F_{j,y,q}$	Fished proportion in quarter q of year y for a fully selected age class a of component j, by the directed and round herring bycatch fisheries	-		D21	
Likelihood	$-lnL^{Nov}$	Contribution to the negative log likelihood from the model fit to the November survey biomass data	-		D32	
	$-lnL^{rec}$	Contribution to the negative log likelihood from the model fit to the recruit survey data	-		D33	
	$-lnL^{surpropl}$	Contribution to the negative log likelihood from the model fit to the November survey proportion-at-length data	-		D34	
	$-lnL^{compropl}$	Contribution to the negative log likelihood from the model fit to the quarterly commercial proportion-at-length data	-		D35	
	$-lnL^{surprev}$	Contribution to the negative log likelihood from the model fit to the November parasite prevalence-at-length data	-		D36	
	ϕ^{S}_{ac}	CV associated with factors which cause bias in the acoustic survey estimates and which vary inter-annually rather than remain fixed over time	-	=0.227		Appendix B of de Moor and Butterworth (2016)
	$\left(\lambda^{S}_{j,N/r}\right)^2$	Additional variance (over and above $\left(\sigma^{S}_{j,y,Nov/rec}\right)^2$ and $(\phi^{S}_{ac})^2$) associated with the November/recruit surveys of component j	-	$U(0,10)$		

Table D1 (Continued).

Parameter / Variable	Description	Units / Scale	Fixed Value / Prior Distribution	Equation	Notes
w_{propl}^{sur}	Weighting applied to the remaining survey proportion-at-length data	-	$= 0.5 \times 0.167$		To allow for autocorrelation[13]
$\sigma_{j,sur}^{S}$	Standard deviation associated with the survey proportion-at-length data of component j	-	$\sqrt{\frac{\sum_{y=y_1}^{y_n} \sum_{l=6^-}^{21^+} \left(\sqrt{\hat{p}_{j,y,l}^{S}} - \sqrt{p_{j,y,l}^{S}}\right)^2}{\sum_{y=y_1}^{y_n} \sum_{l=6^-}^{21^+} 1}}$ [14]		Closed form solution
w_{propl}^{com}	Weighting applied to the commercial proportion-at-length data		$= 0.5 \times 0.04$		To allow for autocorrelation[15]
$\sigma_{j,com}^{S}$	Standard deviation associated with the commercial proportion-at-length data of stock j	-	$\sqrt{\frac{\sum_{y=y_1}^{y_n} \sum_{q=1}^{4} \sum_{l=6}^{23^+} \left(\sqrt{\hat{p}_{j=1,y,q,l}^{comlS}} - \sqrt{\cdots}\right.}{\sum_{y=y_1}^{y_n} \sum_{q=1}^{4} \sum_{l=6}^{23^+} 1}}$ $\sqrt{\frac{\sum_{y=y_1}^{y_n} \sum_{q=1}^{4} \sum_{l=13}^{23^+} \left(\sqrt{\hat{p}_{j=2,y,q,l}^{comlS}} - \sqrt{\cdots}\right.}{\sum_{y=y_1}^{y_n} \sum_{q=1}^{4} \sum_{l=13}^{23^+} 1}}$	Closed form solution[16]	$\sigma_{j,com}^{S}$

[13] Based upon data being available ~6 times more frequently than annual age data which contain maximum information content on this.
[14] The 21^+ group in this equation consists of the length classes 21cm, 21.5cm, 22cm, 22.5cm, 23cm and 23.5cm.
[15] Based upon data being available ~4x6 times more frequently than annual age data which contain maximum information content on this.
[16] A shorter range of lengths is used for the south component given the near absence of data outside this range, resulting in small/zero residuals, which would negatively bias this estimate.

Table D2. Assessment model data, detailed in de Moor *et al*. (2019).

Quantity	Description	Units / Scale	Shown in Figure
t_y^S	Time lapsed between 1 May and the start of the recruit survey in year y	Months	
$\tilde{C}_{j,y,0bs}^S$	Number of juveniles of component j caught between 1 May and the day before the start of the recruit survey in year y	Billions	
$C_{j,y,m,l}^{RLF,fleet}$	Number of fish in length class l landed by $fleet$ in month m of year y of component$j$. $fleet = 1$ denotes the sardine directed fishery, $fleet = 2$ denotes the sardine bycatch with round herring (1984-2011) or ≥14cm sardine bycatch (2012-18) and $fleet = 3$ denotes the juvenile sardine bycatch with anchovy (1984-2011) or <14cm sardine bycatch (2012-18)	Billions	
$\hat{B}_{j,y}^S$	Acoustic survey estimate of biomass of component j from the November survey in year y	Thousand tons	Fig. E1
$\sigma_{j,y,Nov}^S$	Survey sampling CV associated with $\hat{B}_{j,y}^S$ that reflects survey inter-transect variance	-	Fig. E1
$\hat{N}_{j,y,r}^S$	Acoustic survey estimate of recruitment of component j from the recruit survey in year y	Billions	Fig. E2
$\sigma_{j,y,rec}^S$	Survey sampling CV associated with $\hat{N}_{j,y,r}^S$ that reflects survey inter-transect variance	-	Fig. E2
$\hat{p}_{j,y,l}^S$	Observed proportion (by number) of component j in length group l in the November survey of year y	-	Fig. E6
$\hat{p}_{j,y,q,l}^{S,com}$	Observed proportion (by number) of the directed catch and round herring bycatch of fish of component j and length group l during quarter q of year y	-	Fig. E9
$n_{j,y,l}^{prev}$	Number of sardine of component j in length class l sampled from the November survey in year y that were tested and found to be infected with the endoparasite	Numbers	Fig. E12
$N_{j,y,l}^{prev}$	Number of sardine of component j in length class l sampled from the November survey in year y that were tested for infection with the endoparasite	Numbers	Fig. E12

Appendix E. Results from the assessment detailed in Appendix D (from de Moor 2019c).

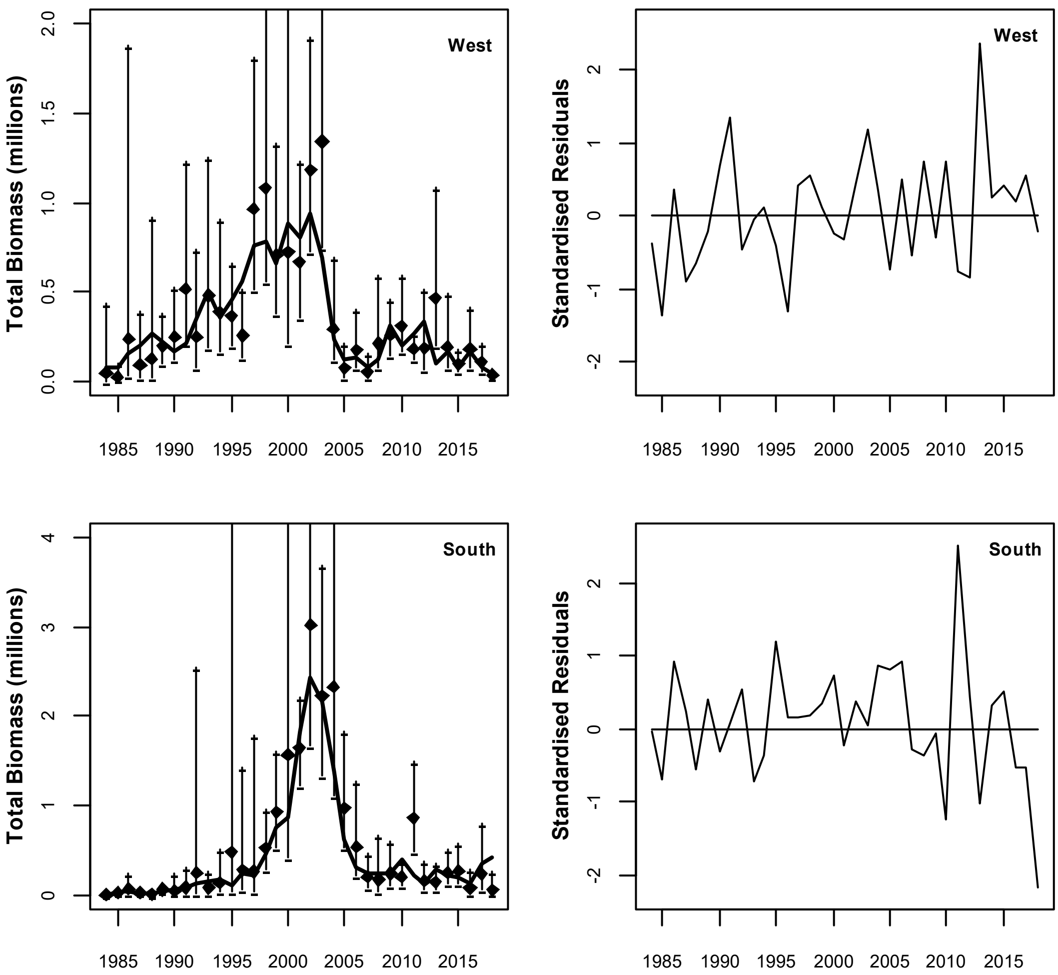

Figure E1. Acoustic survey estimated and model predicted November sardine total biomass from 1984 to 2018. The observed indices are shown with 95% confidence intervals. The standardised residuals (i.e. the residual divided by the corresponding standard deviation, including additional variance where appropriate) from the fits are given in the right hand plots.

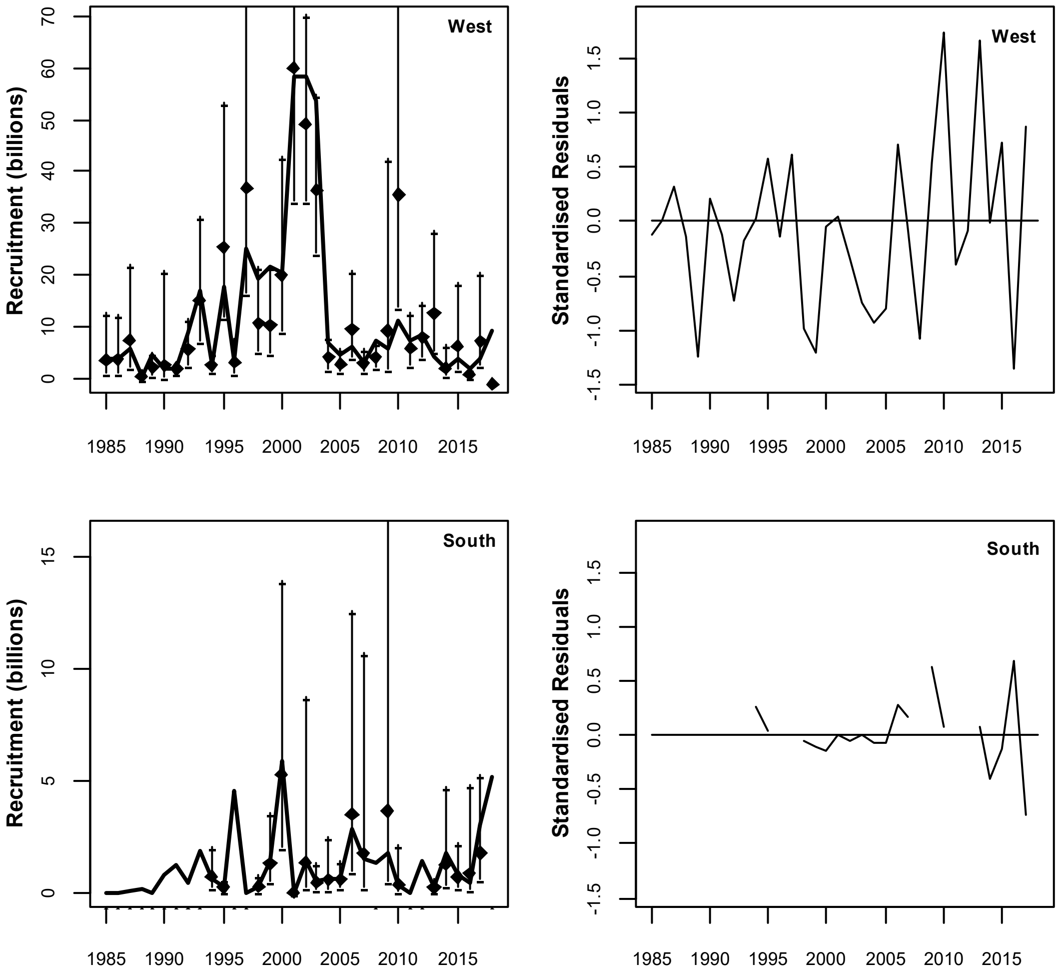

Figure E2. Acoustic survey estimated and model predicted sardine recruitment numbers from May 1985 to May 2018. The survey indices are shown with 95% confidence intervals. The standardised residuals from the fit are given in the right hand plots.

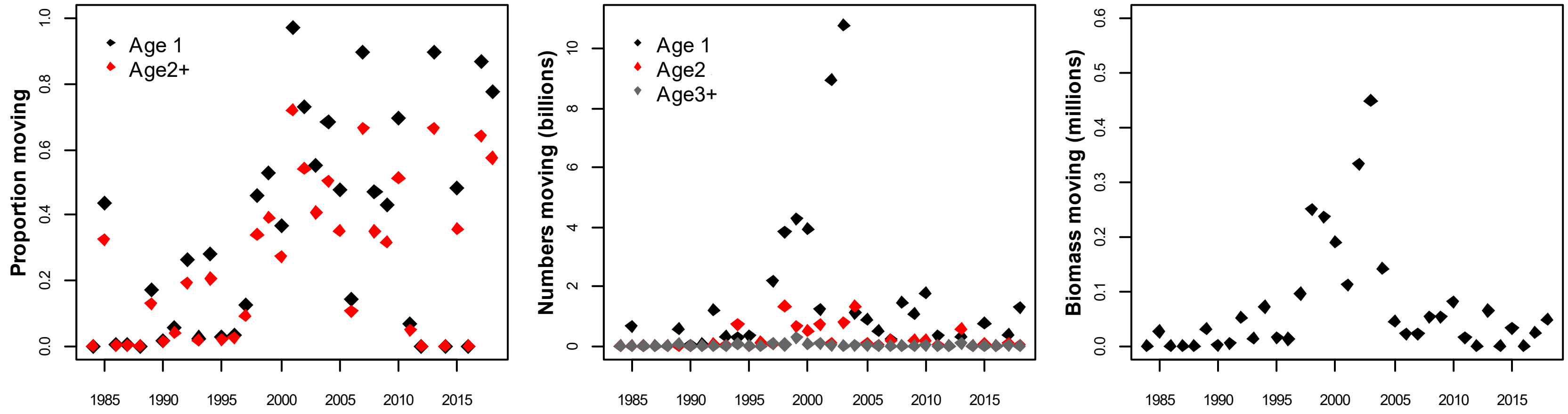

Figure E3. Model estimated proportion of 1-year-olds and 2+-year-olds which move from the "west" component to the "south" component in November. The middle plot shows the numbers of 1-, 2- and 3-year olds moving while the right hand plot shows rough estimates of the annual biomass moving from the west to south component.

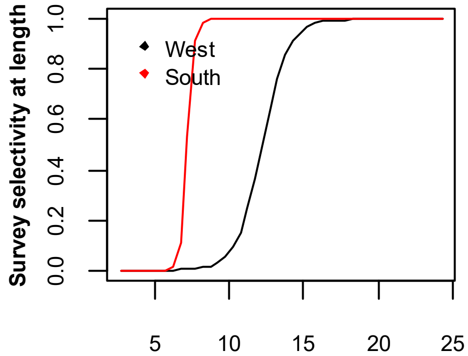

Figure E4. The model estimated November survey selectivity at length.

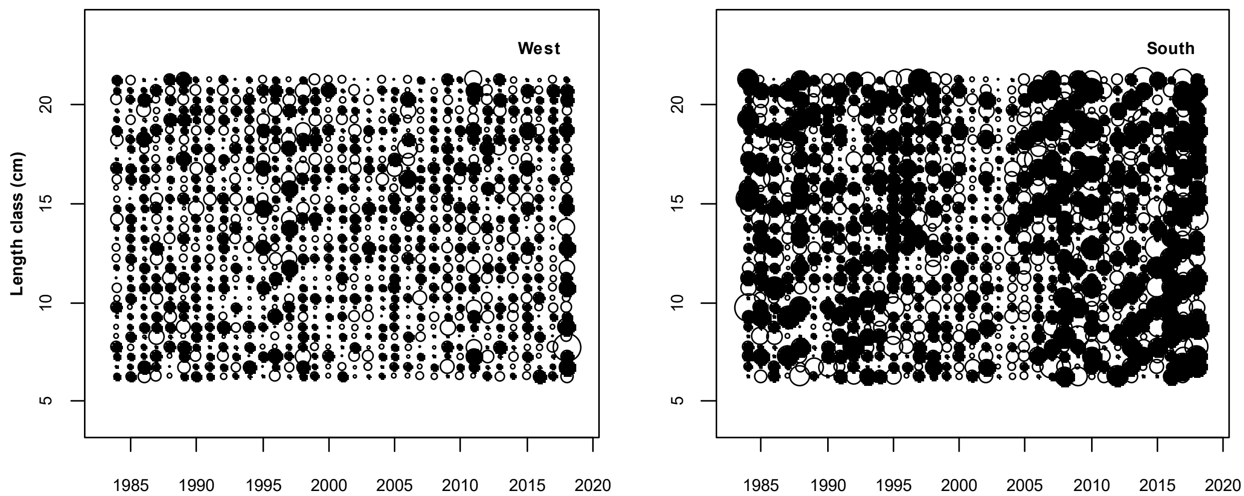

Figure E5. Residuals from the fit of the model predicted proportions-at-length in the November survey to the hydroacoustic survey estimated proportions.

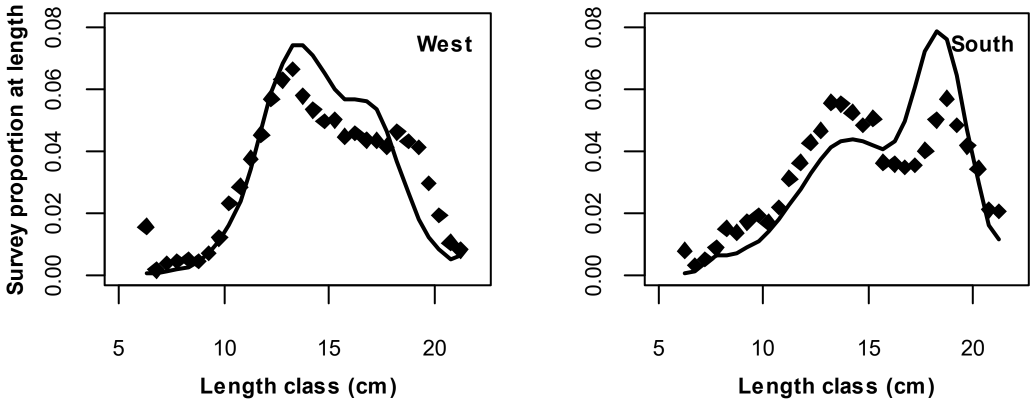

Figure E6. Average (over all years) model predicted and observed proportion-at-length in the November survey.

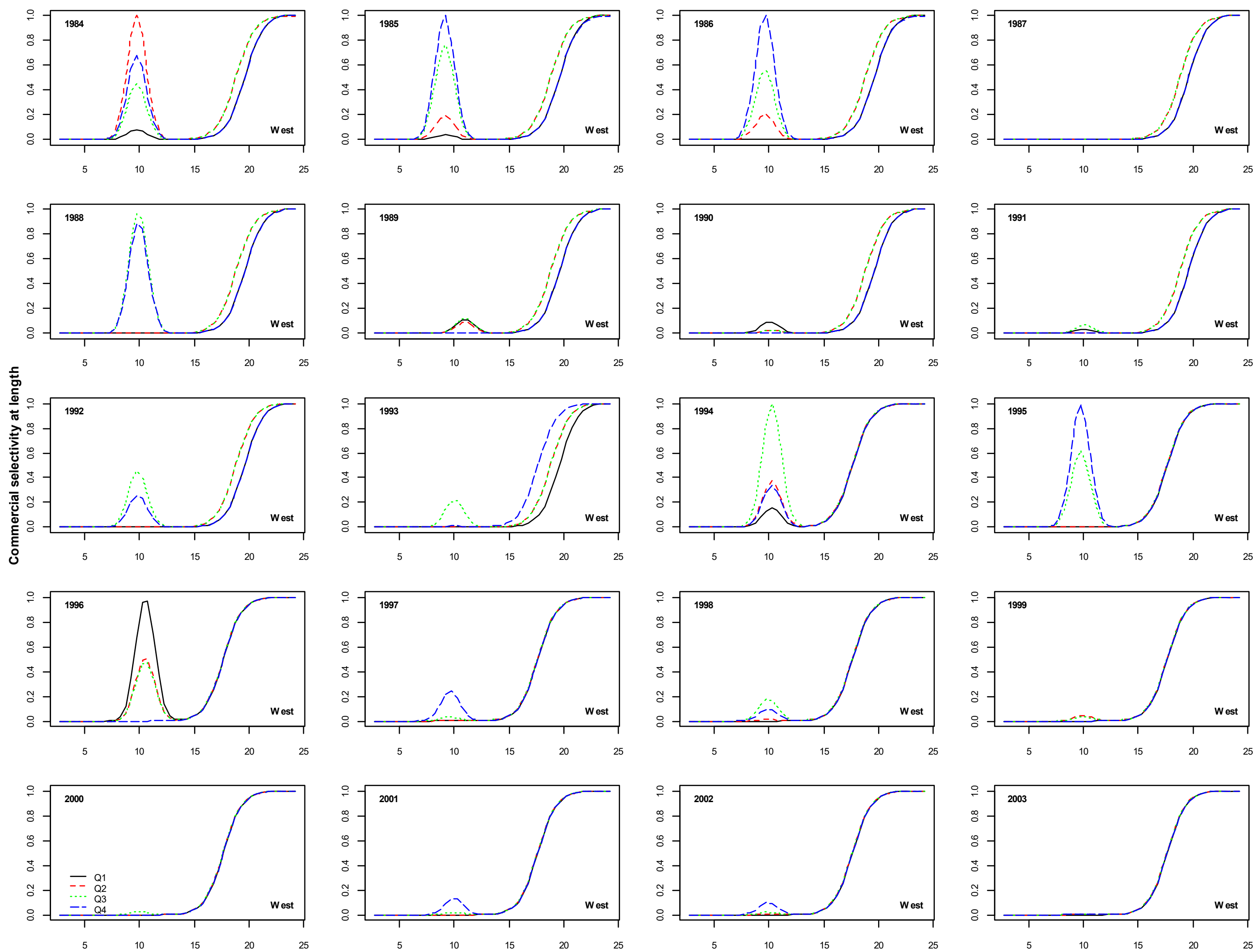

Figure E7. The model estimated commercial selectivity at length.

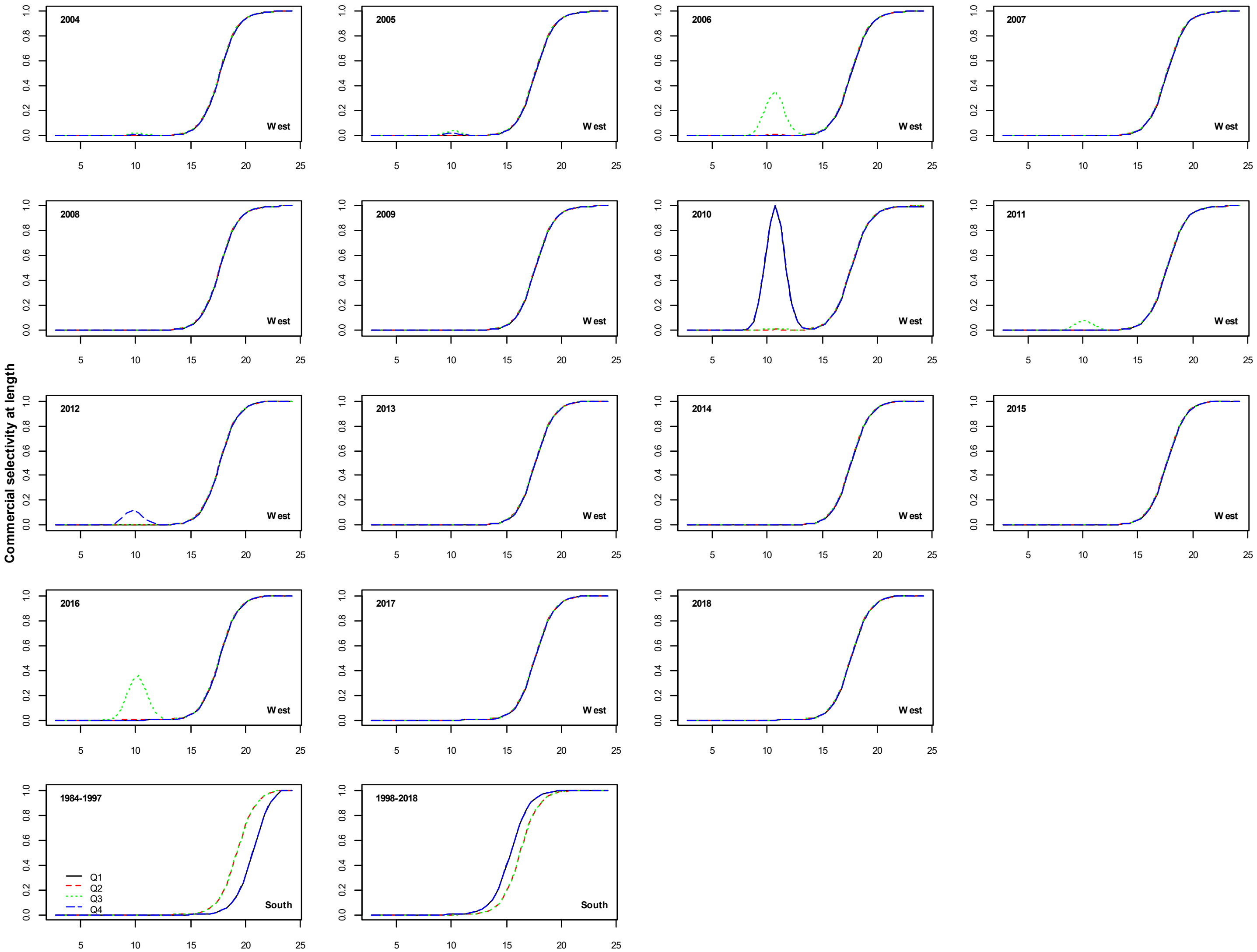

Figure E7 (continued).

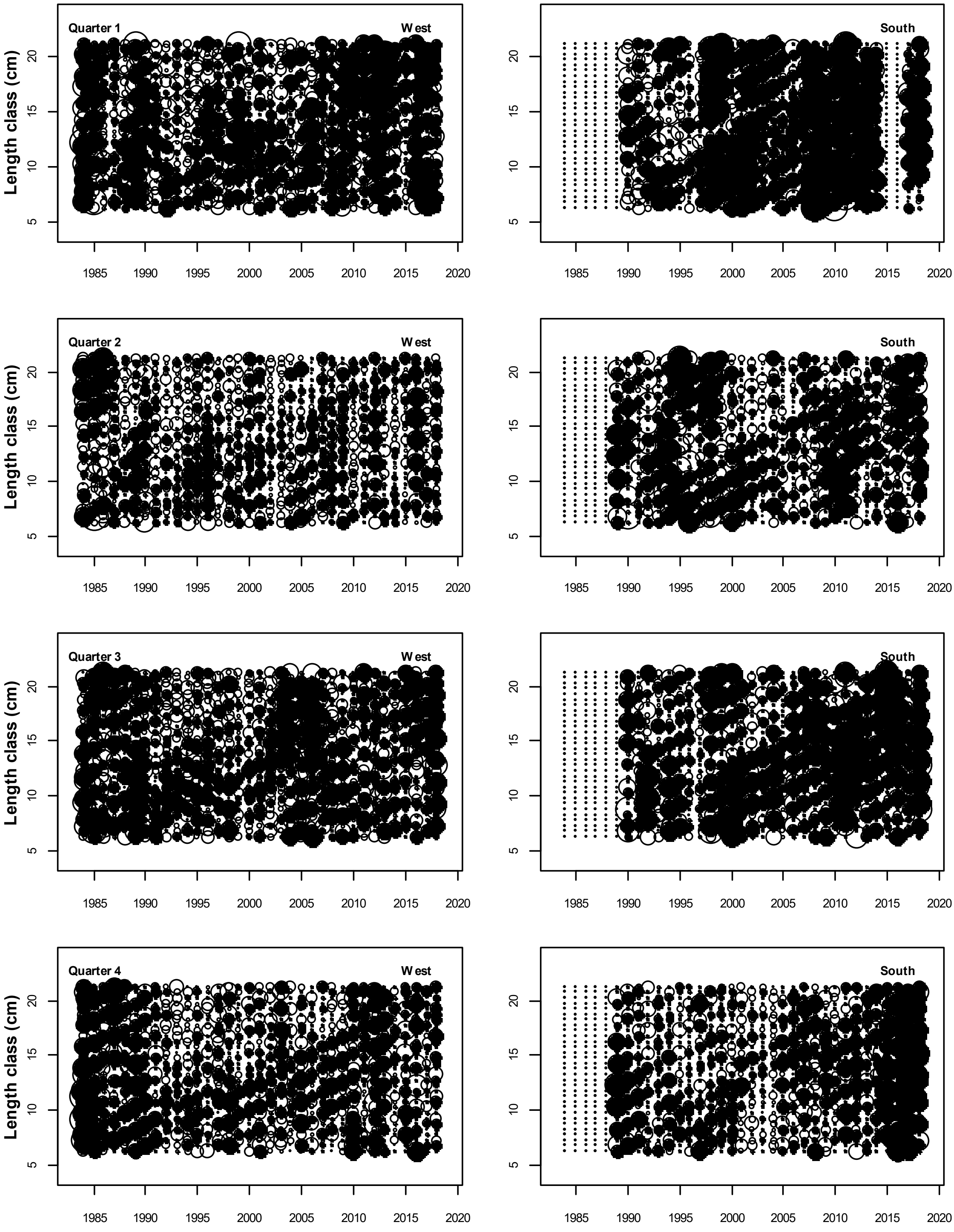
Quarter 1
West
South
Quarter 2
Quarter 3
Quarter 4
Length class (cm)
5
10
15
20
1985
1990
1995
2000
2005
2010
2015
2020

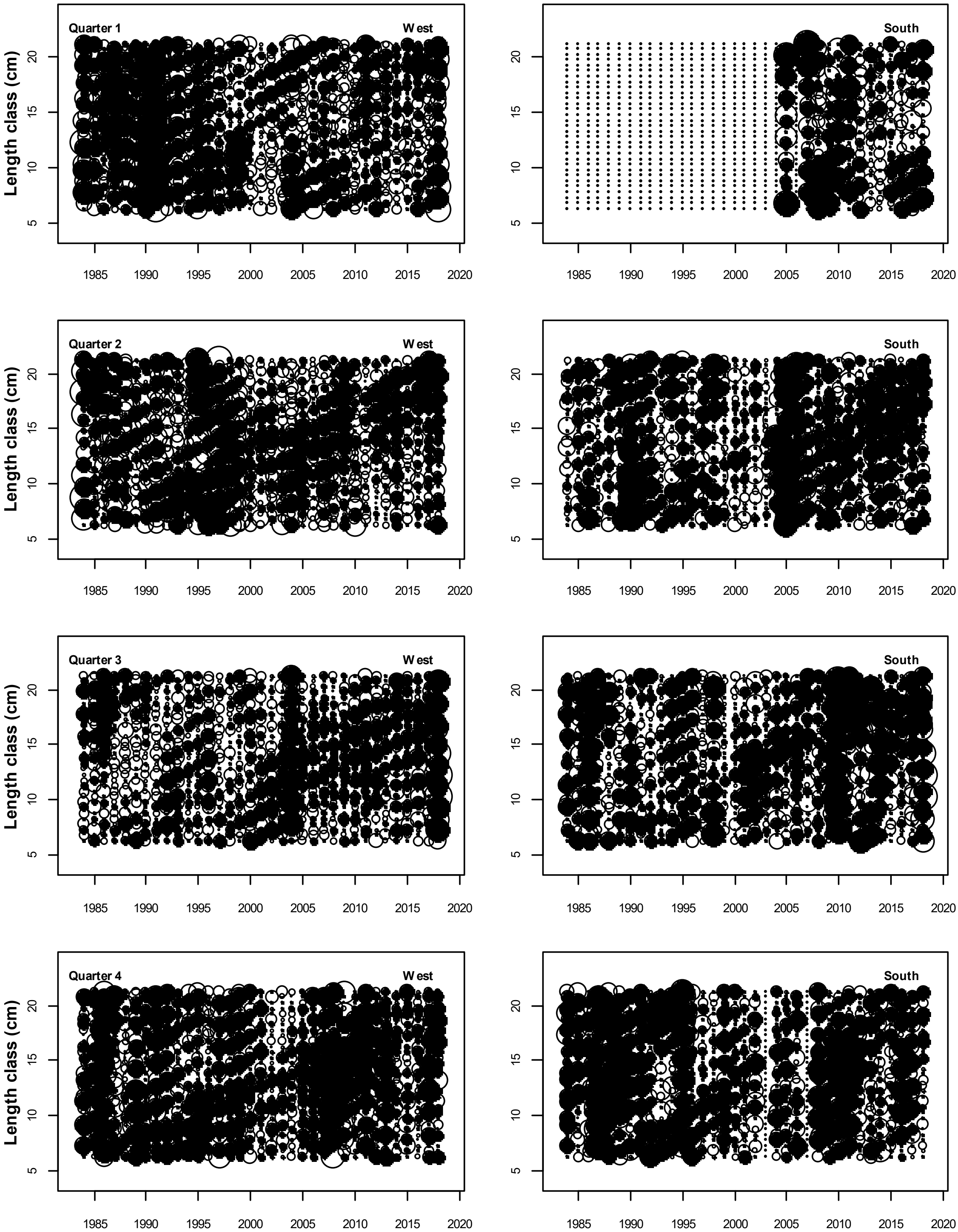

Figure E8. Residuals from the fit of the model predicted proportions-at-length in the quarterly commercial catch to the observed proportions.

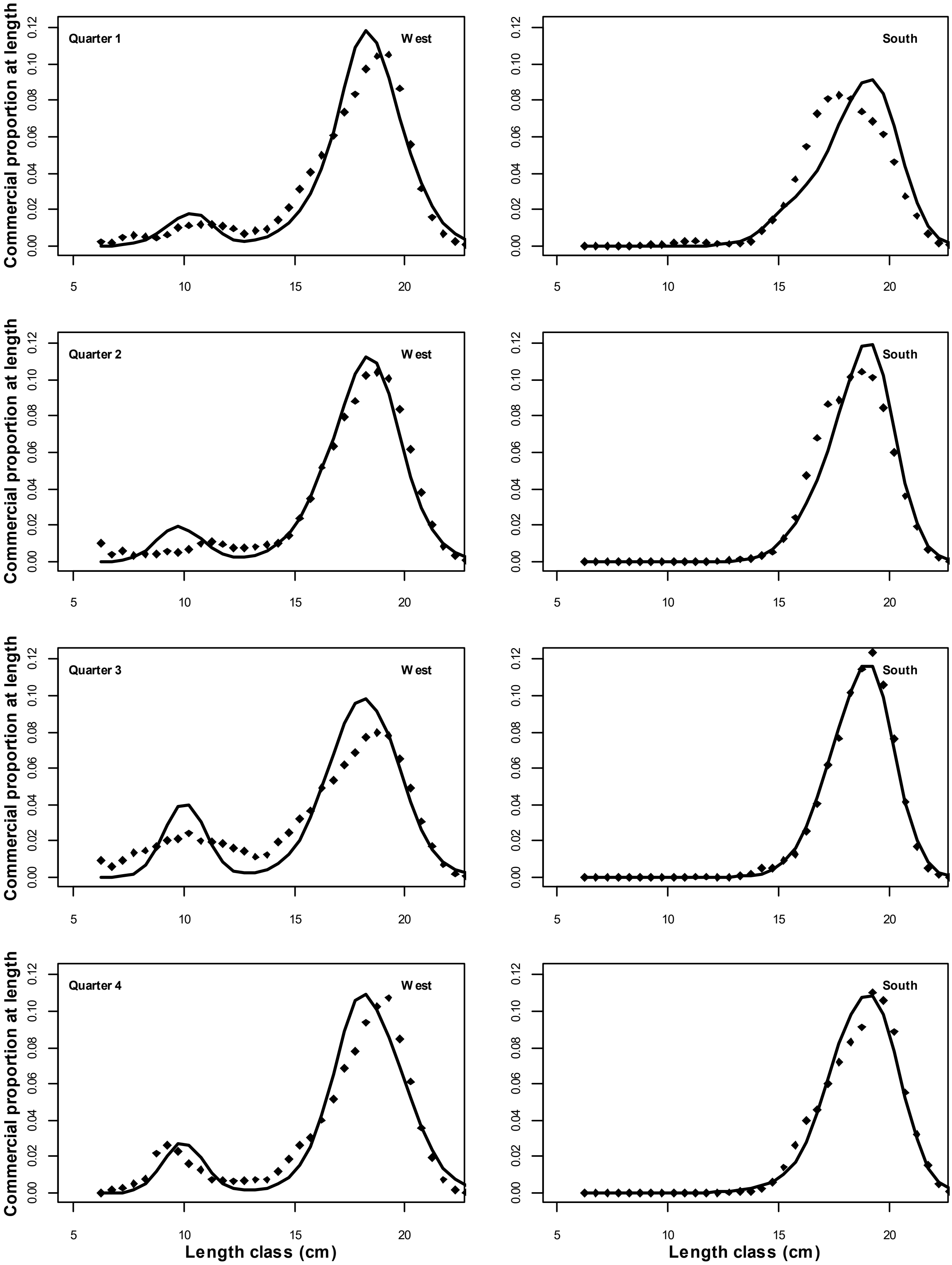
Quarter 1
West
South
Quarter 2
West
South
Quarter 3
West
South
Quarter 4
West
South
Commercial proportion at length
Length class (cm)
0.00
0.02
0.04
0.06
0.08
0.10
0.12
5
10
15
20

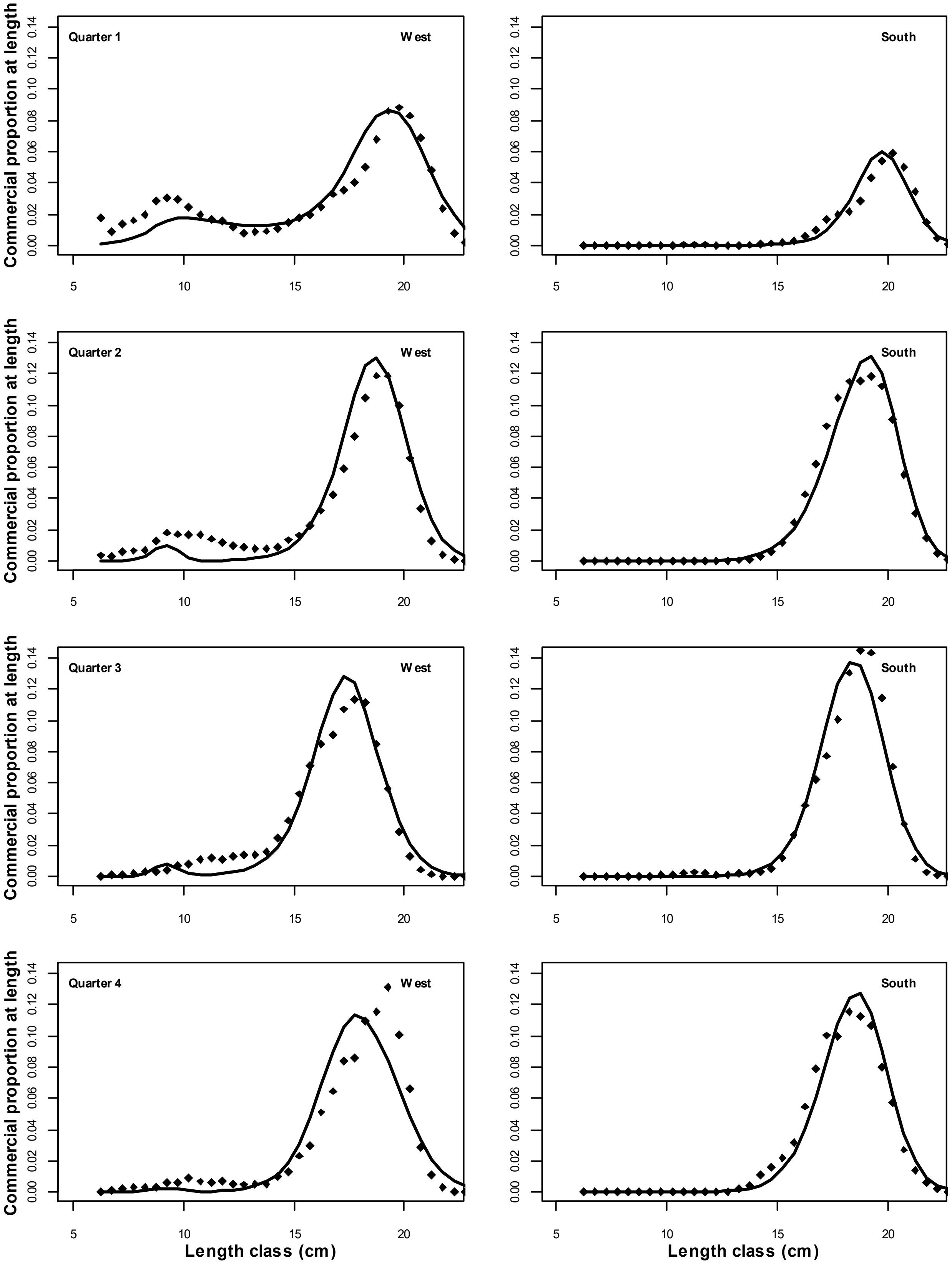

Figure E9. Average (over all quarters and years) model predicted and observed proportion-at-length in the commercial catch (top row), and average (over all years) quarterly model predicted and observed proportions-at-length in the commercial catch (subsequent rows). See Appendix B of de Moor (2019c) for plots for each year and quarter

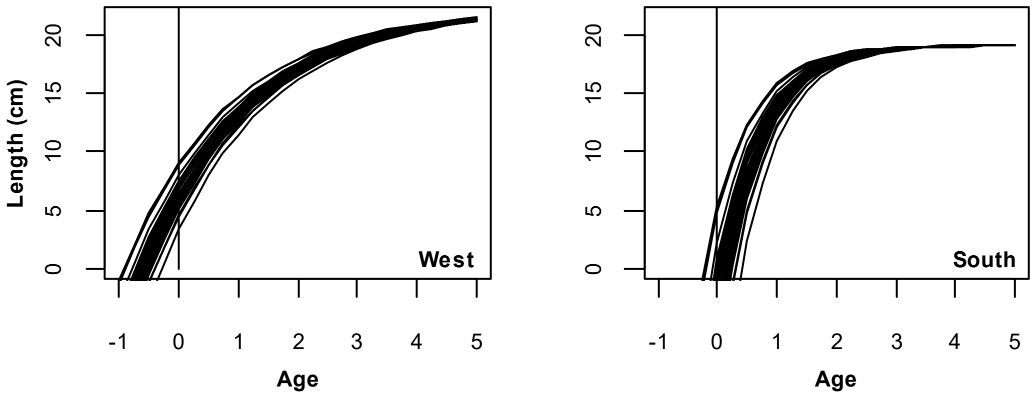

Figure E10. The annual von Bertalanffy growth curves estimated by allowing for auto-correlated residuals for the variation about the age at which length is zero.

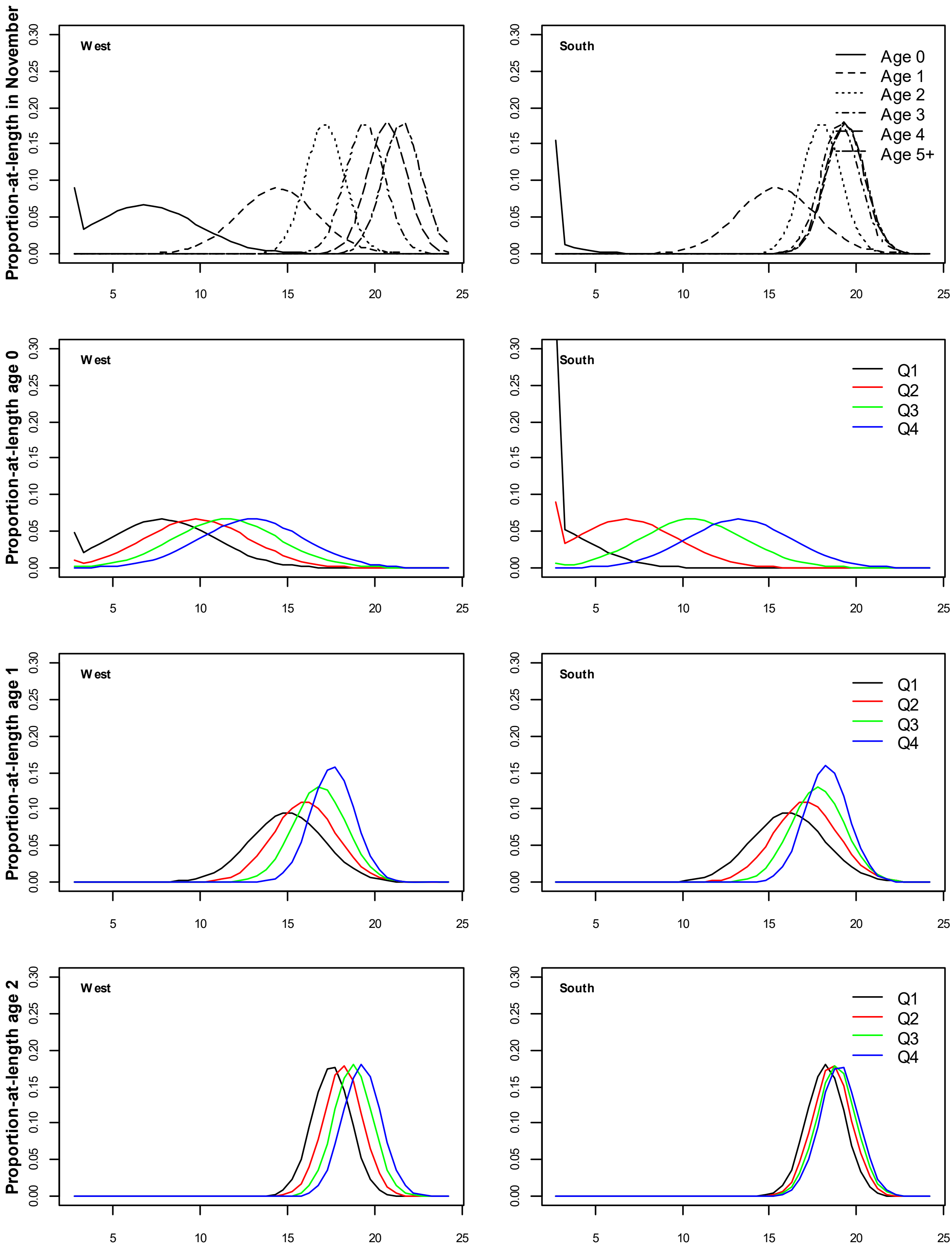

Figure E11. The model estimated distributions of proportions-at-length for each age **in 2010**, given at the time of the biomass survey (1 November, top row), and middle of each quarter of the year (corresponding to the times commercial catch is modelled to be taken) for age 0, 1 and 2 (subsequent rows).

Figure E12. The model estimated proportion of west component sardine infected with the parasite between 2008 and 2018. (Annual infection rate is arbitrarily assumed to be 0 prior to 2008.)

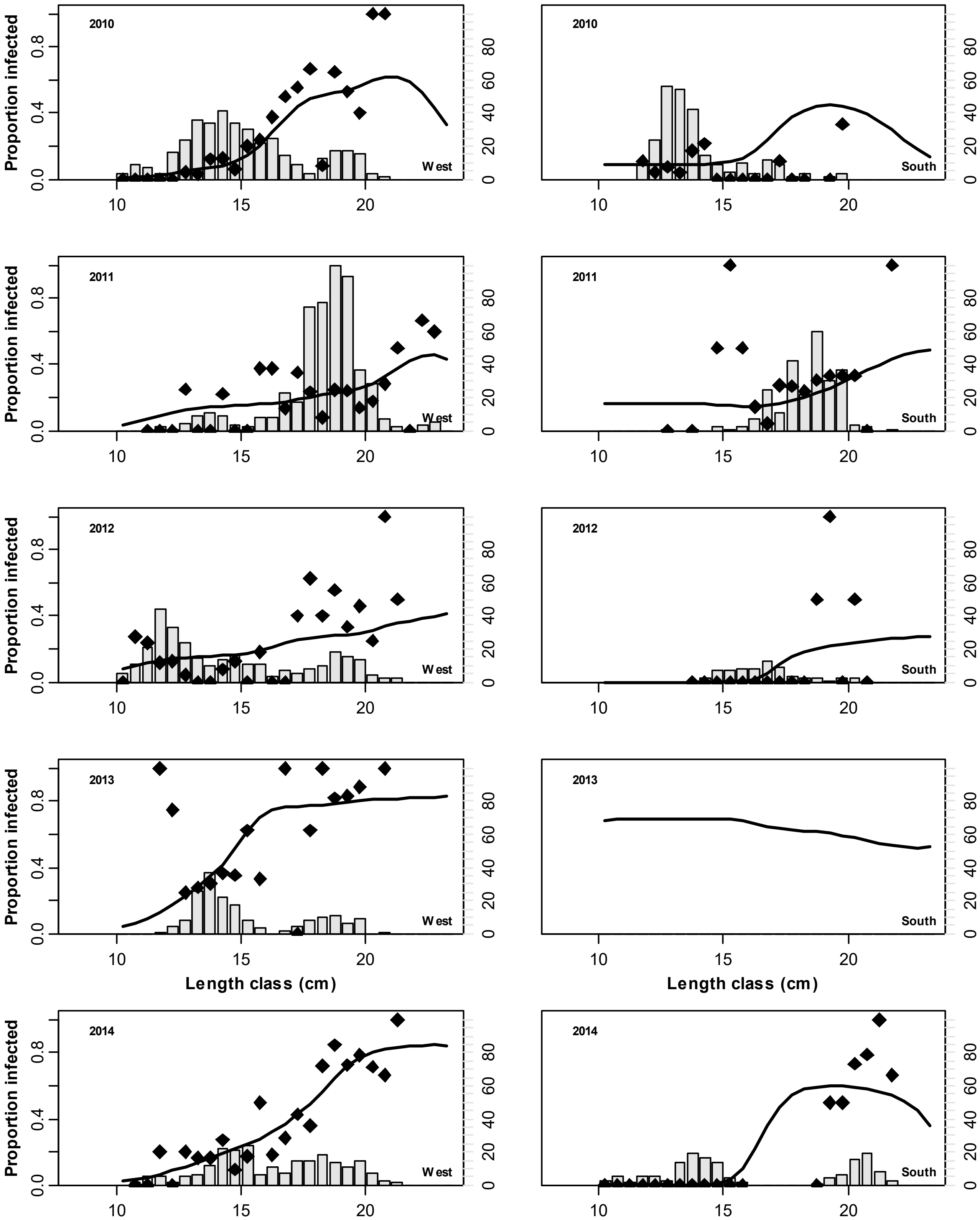

Figure E13. The model estimated proportions-at-length of west and south stock sardine infected with the parasite (i.e. parasite prevalence-by-length) between 2010 and 2018 together with the observed proportions-at-length. The sample size for each length class is given by the grey bars, plotted against the right vertical axis.

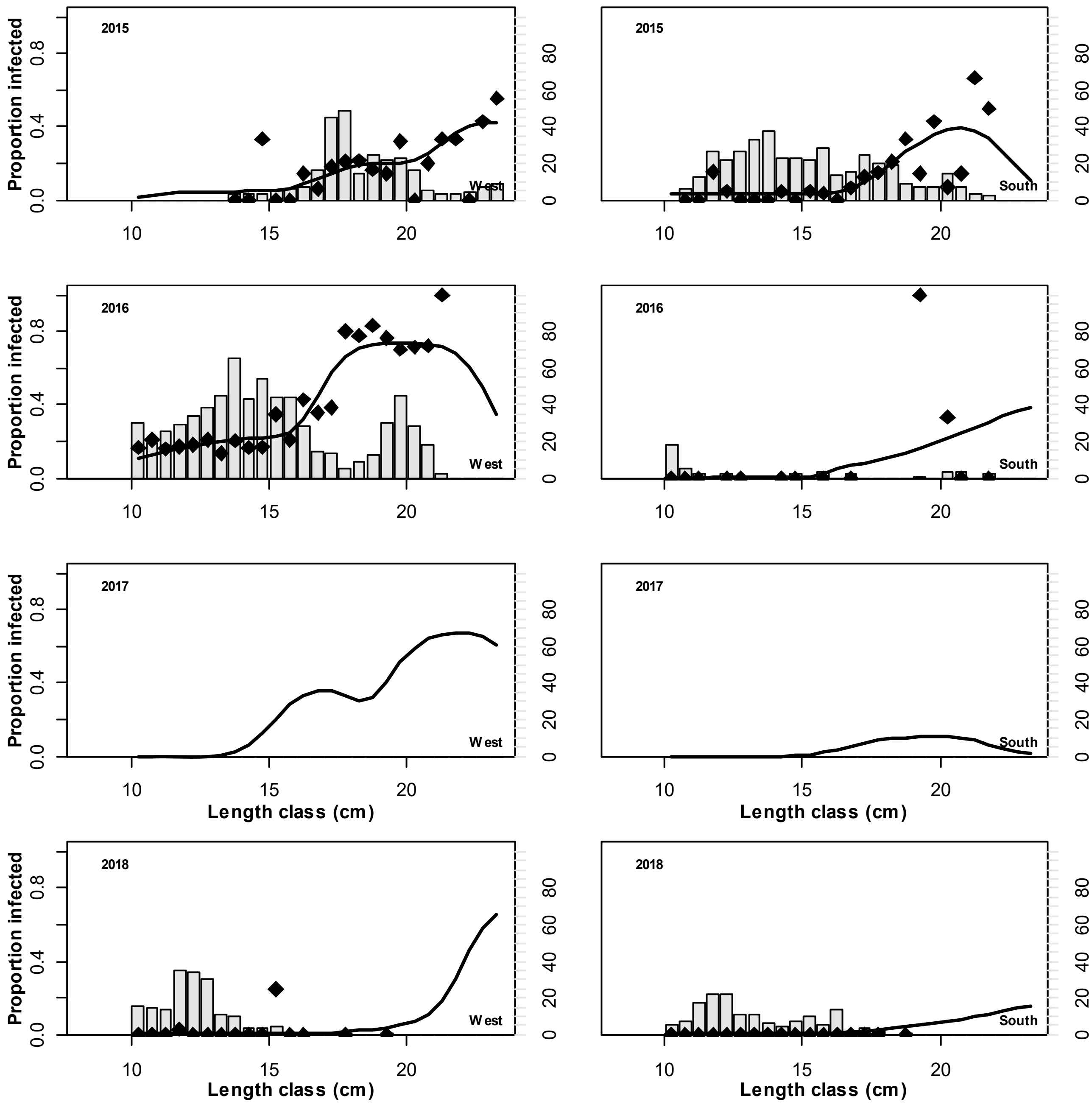

Figure E13 (continued).

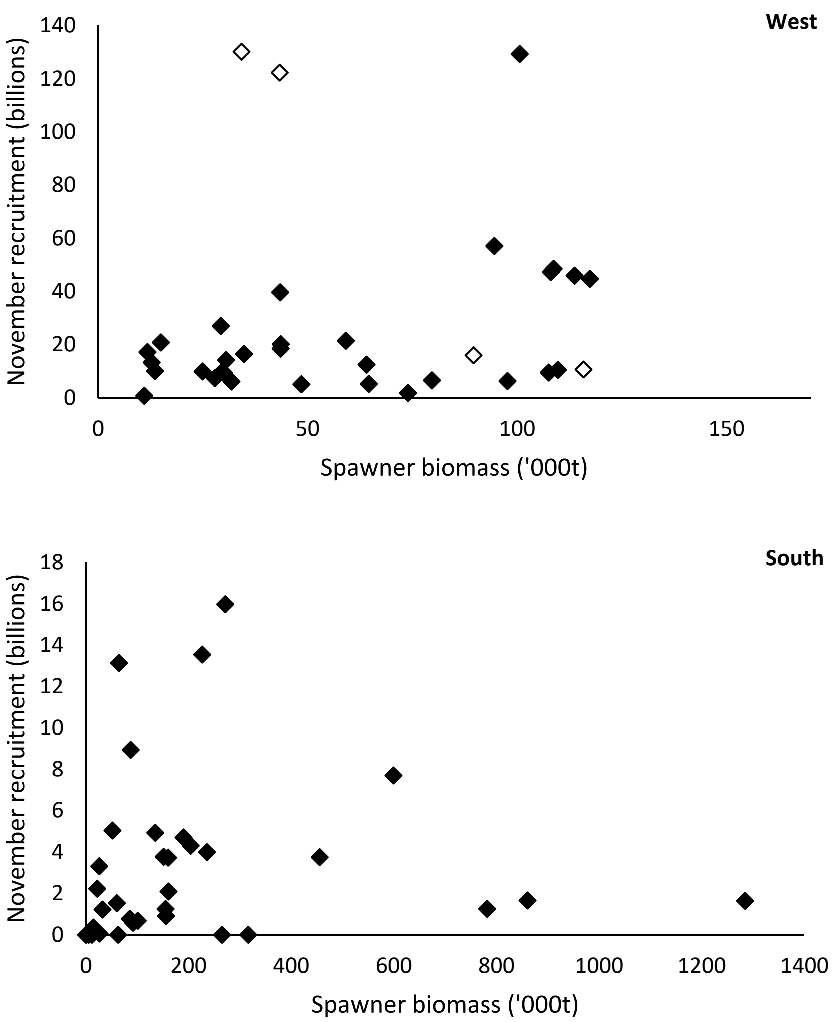

Figure E14. Model predicted sardine recruitment (in November) plotted against spawner biomass from November 1983 to November 2017.

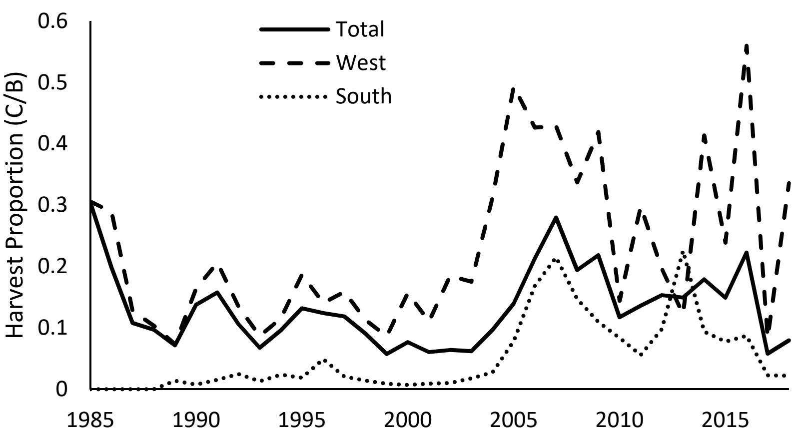

Figure E15. The exploitation rate (simply calculated as the observed annual (Nov-Oct) catch tonnage as a proportion of the model predicted total biomass).

Appendix F: Baseline projections using constant catch assumptions

The projections will be run from November $y_1 = 2019$ to November $y_n = 2040$. The notation is the same as that of Appendix D and Tables D1 and D2. The following assumptions were made:

- The numbers-at-age are calculated as follows:

$$N_{j,p,y,a}^{S*} = \left(N_{j,p,y-1,a-1}^{S} e^{-M_{y,a-1}^{S}/2} - C_{j,p,y,a-1}^{S}\right) e^{-M_{y,a-1}^{S}/2} \qquad p = I, NI, y_1 \le y \le y_n,\ 1 \le a \le 5^{+} \qquad \text{(F1)}$$

$$N_{j,p,y,5^+}^{S*} = \left(N_{j,p,y-1,4}^{S} e^{-M_{y,4}^{S}/2} - C_{j,p,y,4}^{S}\right) e^{-M_{y,4}^{S}/2} + \left(N_{j,p,y-1,5^+}^{S} e^{-M_{y,5^+}^{S}/2} - C_{j,p,y,5^+}^{S}\right) e^{-M_{y,5^+}^{S}/2}$$
$$p = I, NI, y_1 \le y \le y_n \qquad \text{(F2)}$$

 and

$$\mathrm{N}_{\mathrm{W,p,y,a}}^{\mathrm{S}} = \left(1 - \mathrm{move}_{\mathrm{y,a}}\right) \mathrm{N}_{\mathrm{W,p,y,a}}^{\mathrm{S**}} \qquad p = I, NI, y_1 \le y \le y_n,\ 1 \le a \le 5^{+}$$
$$\mathrm{N}_{\mathrm{S,p,y,a}}^{\mathrm{S}} = \mathrm{N}_{\mathrm{S,p,y,a}}^{\mathrm{S**}} + \mathrm{move}_{\mathrm{y,a}} \mathrm{N}_{\mathrm{W,p,y,a}}^{\mathrm{S**}} \qquad p = I, NI, y_1 \le y \le y_n,\ 1 \le a \le 5^{+} \qquad \text{(F3)}$$

- Future infection is assumed to be zero (this is inconsequential to projections).
- Future movement of 1-year olds from the west to the south component is assumed to be time-invariant and $\mathrm{move}_{\mathrm{y,1}}$ =0.3[17]. Additionally, if a density-dependent hypothesis were assumed (de Moor e*t al.* 2018), one would expect movement in the short-term to be relatively low.
- Future recruitment is generated from the past 5[18] years of recruitment under the assumption that future recruitment, particularly in the immediate short-term future, may be from a similar 'regime' to that of the more recent 5 years. For example, recruitment may depend more on environmental conditions rather than on spawning stock biomass (Szuwalski *et al*. 2019). Autocorrelation in the historical recruitment time series is non-negligible lending further weight to this being a preferred baseline choice for these analyses.
- Natural mortality is assumed to be time-invariant: $M_{y,a=0}^{S} = \bar{M}_{ju}^{S}$ and $M_{y,a=1+}^{S} = \bar{M}_{ad}^{S}$
- No allowance is made for early/late recruitment in future years, i.e. $\varepsilon_y^t = 0$ in equation (D8).
- Growth curves at the mid-point of each quarter (equation D16) and therefore the quarterly commercial selectivity-at-age functions (equation D15) were the same[19] for all future years.
- Growth curves in November (equation D7) were thus also the same for all future years.
- Only the logistic part of the selectivity-at-length curve is used for future projections of alternative directed catches. Small sardine bycatch with directed >14cm sardine is assumed to consist of recruits-of-the-year.
- Future annual selectivity-at-age is assumed to be time-invariant and averaged over all quarters of the most recent commercial selectivity-at-length estimated from 2002-2019 (note growth curves are time-invariant in future years):

$$S_{j,a}^{S} = 0.25 \textstyle\sum_{q=1}^{4} \sum_{l=2.5^-}^{24^+} A_{j,2019,q,a,l}^{com} S_{j,2018,q,l} = 0.25 \ \ 0 \le a \le 5^{+} \qquad \text{(F4)}$$

- The numbers-at-length are calculated according to equations (D5) and (D6).
- The same maturity-at-length relationship, based on that corresponding to the period 1965-1975, is assumed from 2004 onwards, for all projected years.

---

[17] It will be confirmed that this value remains close to the average of the recent past once the assessment is updated with 2019 data.

[18] The most recent 5 or 10 years are frequent choices for the "recent past" in projection analyses internationally.

[19] Except in cases where the selectivity is modified to allow catch to be spread to lower ages (described below).

- The November biomass, spawner biomass and effective spawner biomass are calculated according to equations (D11) to (D13).
- A time-invariant but component-dependent November weight-at-length relationship is assumed (analyses in progress).
- Catch weight-at-age is taken to be the average of the weight-at-age in November immediately before and after the pulse fishery is assumed, i.e.

$w_{j,y,a}^{catch} = 0.5\left(w_{j,,a}^{S} + w_{j,a+1}^{S}\right) \quad 0 \le a \le 4$

$$w_{j,y,5^+}^{catch} = w_{j,,5^+}^{S} \tag{F5}$$

where

$$w_{j,y,a}^{S} = \sum_{l=2.5^-}^{l=24^+} A_{j,y,a,l}^{sur} w_{j,y,l}^{S} \tag{F6}$$

- Catch is assumed to be taken in a single pulse, mid-way through the year. Bycatch is calculated as:

$$C_{j,p,y,a}^{bycatch} = \frac{Bycatch}{\sum_{a=0}^{1}\sum_{p=I,NI} N_{j,p,y-1,a}^{S} e^{-M_{y,a}^{S}/2} w_{j,a}^{catch}} \times N_{j,p,y-1,a}^{S} e^{-M_{y,a}^{S}/2} \le N_{j,p,y-1,a}^{S} e^{-M_{y,a}^{S}/2}$$

And directed catch (taken to include large sardine bycatch) is calculated as:

$$C_{j,p,y,a}^{dir} = \frac{Directed+Large\ Bycatch}{\sum_{a=0}^{5^+}\sum_{p=I,NI}\left(N_{j,p,y-1,a}^{S} e^{-M_{y,a}^{S}/2} - C_{j,p,y,a}^{bycatch}\right) S_{j,a}^{S} w_{j,a}^{catch}} \times \left(N_{j,p,y-1,a}^{S} e^{-M_{y,a}^{S}/2} - C_{j,p,y,a}^{bycatch}\right) S_{j,a}^{S} \text{ , with}$$

$$\frac{Directed+Large\ Bycatch}{\sum_{a=0}^{5^+}\sum_{p=I,NI}\left(N_{j,p,y-1,a}^{S} e^{-M_{y,a}^{S}/2} - C_{j,p,y,a}^{bycatch}\right) S_{j,a}^{S} w_{j,a}^{catch}} \times S_{j,5}^{S} \le 0.95$$

$$C_{j,p,y,a}^{S} = C_{j,p,y,a}^{bycatch} + C_{j,p,y,a}^{dir} \qquad p = I, NI, y > y_n, 1 \le q \le 4, 0 \le a \le 5^+ \tag{F7}$$

- In cases where the above constraints would otherwise result in the realised catch being less than the tested scenario, the selectivity is modified as follows:

If $\frac{Directed+Large\ Bycatch}{\sum_{a=0}^{5^+}\sum_{p=I,NI}\left(N_{j,p,y-1,a}^{S} e^{-M_{y,a}^{S}/2} - C_{j,p,y,a}^{bycatch}\right) S_{j,a}^{S} w_{j,a}^{catch}} \times S_{j,5}^{S} \le 0.95$

Then $C_{j,p,y,5+}^{dir} = 0.95\left(N_{j,p,y-1,5+}^{S} e^{-M_{y,5+}^{S}/2} - C_{j,p,y,5+}^{bycatch}\right)$

If $\frac{Directed+Large\ Bycatch}{\sum_{a=0}^{4}\sum_{p=I,NI}\left(N_{j,p,y-1,a}^{S} e^{-M_{y,a}^{S}/2} - C_{j,p,y,a}^{bycatch}\right) S_{j,a}^{S} w_{j,a}^{catch}} \times S_{j,4}^{S} \le 0.95$

Then $C_{j,p,y,4}^{dir} = 0.95\left(N_{j,p,y-1,4}^{S} e^{-M_{y,4}^{S}/2} - C_{j,p,y,4}^{bycatch}\right)$

Else $C_{j,p,y,a<5}^{dir} = \frac{Directed+Large\ Bycatch}{\sum_{a=0}^{3}\sum_{p=I,NI}\left(N_{j,p,y-1,a}^{S} e^{-M_{y,a}^{S}/2} - C_{j,p,y,a}^{bycatch}\right) S_{j,a}^{S} w_{j,a}^{catch}} \times \left(N_{j,p,y-1,a}^{S} e^{-M_{y,a}^{S}/2} - C_{j,p,y,a}^{bycatch}\right) S_{j,a}^{S}$

If $\frac{Directed+Large\ Bycatch}{\sum_{a=0}^{3}\sum_{p=I,NI}\left(N_{j,p,y-1,a}^{S} e^{-M_{y,a}^{S}/2} - C_{j,p,y,a}^{bycatch}\right) S_{j,a}^{S} w_{j,a}^{catch}} \times S_{j,3}^{S} \le 0.95$

Then $C_{j,p,y,3}^{dir} = 0.95\left(N_{j,p,y-1,3}^{S} e^{-M_{y,3}^{S}/2} - C_{j,p,y,3}^{bycatch}\right)$

Else $C_{j,p,y,a<4}^{dir} = \frac{Directed+Large\ Bycatch}{\sum_{a=0}^{3}\sum_{p=I,NI}\left(N_{j,p,y-1,a}^{S} e^{-M_{y,a}^{S}/2} - C_{j,p,y,a}^{bycatch}\right) S_{j,a}^{S} w_{j,a}^{catch}} \times \left(N_{j,p,y-1,a}^{S} e^{-M_{y,a}^{S}/2} - C_{j,p,y,a}^{bycatch}\right) S_{j,a}^{S}$

If $\frac{Directed+Large\ Bycatch}{\sum_{a=0}^{2}\sum_{p=I,NI}\left(N_{j,p,y-1,a}^{S} e^{-M_{y,a}^{S}/2} - C_{j,p,y,a}^{bycatch}\right) S_{j,a}^{S} w_{j,a}^{catch}} \times S_{j,2}^{S} \le 0.95$

Then $C_{j,p,y,2}^{dir} = 0.95\left(N_{j,p,y-1,2}^{S} e^{-M_{y,2}^{S}/2} - C_{j,p,y,2}^{bycatch}\right)$

$$C_{j,p,y,a<2}^{dir} = \frac{Directed+Large\ Bycatch}{\sum_{a=0}^{1}\sum_{p=I,NI}\left(N_{j,p,y-1,a}^{S}e^{-M_{y,a}^{S}/2}-C_{j,p,y,a}^{bycatch}\right)S_{j,a}^{S}w_{j,a}^{catch}} \times \left(N_{j,p,y-1,a}^{S}e^{-M_{y,a}^{S}/2} - C_{j,p,y,a}^{bycatch}\right)S_{j,a}^{S}$$, with

$$\frac{Directed+Large\ Bycatch}{\sum_{a=0}^{1}\sum_{p=I,NI}\left(N_{j,p,y-1,a}^{S}e^{-M_{y,a}^{S}/2}-C_{j,p,y,a}^{bycatch}\right)S_{j,a}^{S}w_{j,a}^{catch}} \times S_{j,5}^{S} \leq 0.95$$ [20]

[20] There are still a few cases where the full catch is not realised by this equation reaching the constraint, even after the modifications to the selectivity are done.